Title

Nutrient deposition and alteration of food web structure in high-elevation lakes of the Sierra Nevada: response by microbial communities

Authors

Nelson, Craig E
Carlson, Craig A
Melack, John M

Publication Date

2008

Nutrient deposition and alteration of food web structure in high-elevation lakes of the Sierra Nevada: response by microbial communities

Craig E. Nelson

Craig A. Carlson

John M. Melack

Marine Science Institute, University of California, Santa Barbara, 93106

University of California Water Resources Center
Technical Completion Report
Project W-988
January 2008

Please direct correspondence to:
Craig E. Nelson, Department of Ecology, Evolution and Marine Biology,
University of California, Santa Barbara, CA, 93106-9610
cr_nelson@lifesci.ucsb.edu

Acknowledgements: We thank the following individuals for assisting with various aspects of field and laboratory studies: Kevin Skeen, Steven Sadro, Frank Setaro, Janice Jones, William Clinton, and Anya Engen. James Sickman, Roland Knapp, Scott Cooper and Sally MacIntyre contributed valuable insight into study design and interpretation. We also wish to thank the following agencies for logistical support and ancillary data: UCSB Marine Science Institute, California Department of Fish and Game, Yosemite and Sequoia-Kings Canyon National Parks, USGS, Inyo and El Dorado National Forests, Sierra Nevada Aquatic Research Laboratory. Additional financial support was provided by NSF grants DEB0089839 and DEB0614207 to JMM.

Executive Summary

There are more than 4000 lakes above 2500 m elevation in the Sierra Nevada of California. Recent developments in understanding of aquatic ecosystem function predict that metabolism and food web structure in these dilute, low-productivity lakes may be dominated by an active and diverse microbial community. The identity, activity, and importance of pelagic prokaryotic communities (bacterioplankton) in these ecosystems is little known, yet understanding the role of these organisms in lake metabolism and food web dynamics is critical to predicting the response of Sierra lakes to global change. This study combined range-wide surveys, multiannual seasonal monitoring, and experimental approaches to describe the biodiversity and biogeochemical role of bacterioplankton in high-elevation lakes of the Sierra Nevada. Particular attention was payed to determining the impacts of anthropogenic nutrient deposition and introduced salmonids on the structure and metabolism of microbial communities.

Our results indicate an abundant, remarkably diverse, and metabolically active bacterioplankton community. A three-year study of Emerald Lake, a representative cirque lake in Sequoia National Park, provided estimates of more than 250 bacterial phylotypes exhibiting predictable patterns of community phenology in response to seasonal transitions. Bacterial densities averaged 1 billion cells per liter throughout the year, and estimates of bacterioplankton biomass averaged 40% of total pelagic biomass. Rates of bacterial production were comparable to rates of net primary production, ranging from 1% during fall phytoplankton blooms to nearly 500% during snowmelt when terrestrial inputs of dissolved organic matter were highest. Bacterial metabolic properties were coupled to larger ecosystem dynamics, with growth efficiencies correlated with rates of primary productivity.

Phosphorus enrichment, but not nitrogen enrichment, produced rapid and sustained increases in bacterial production rates and produced significant alterations to bacterial community structure. The metabolic and community response to nutrient enrichment by the bacterioplankton was independent of phytoplankton responses, suggesting that microbial populations may be more sensitive indicators of eutrophication and ecosystem change. Among lakes throughout the Sierra Nevada, introduced salmonid fish had no significant relationship with multivariate bacterial community composition, but salmonid density did exhibit a significant positive correlation with bacterial phylotype richness and diversity, suggesting that trout introductions have altered bacterioplankton community structure. Within catchments bacterial communities exhibited decreasing similarity with increasing biogeographic distance, supporting the concept that macroecological principles of dispersal and isolation play a role in structuring communities of microorganisms.

This study highlights the importance of bacteria in lake ecosystems of the Sierra Nevada by providing spatially and temporally robust estimates of biomass, metabolism, diversity, and role in ecosystem biogeochemical processes. In addition to specifically defining impacts of introduced species and nutrient enrichment on microbial communities, it provides a sturdy ecological scaffolding for future studies of the role of microorganisms in high-elevation lake ecosystems.

Introduction and Problem Statement

High-elevation lakes of the Sierra Nevada, once considered isolated from human impacts, are increasingly experiencing the effects of population expansion. Nutrient loading, the result of increasing atmospheric deposition, and the stocking of non-native trout, halted in National Parks but continuing on selected Forest Service lands, are major anthropogenic impacts to these remote ecosystems. The ecological impacts of both trout stocking and atmospheric pollutants have been studied in high-elevation lakes of the Sierra for nearly two decades, and have been shown to impose significant and lasting impacts at a regional scale, including eradication of endangered species, alterations to algal productivity, and changes in zooplankton population dynamics. Connecting these shifts to ecosystem function and biogeochemical cycling is necessary for understanding and predicting ecological impacts in these lakes, yet this has not yet been a focus, despite the documented sensitivity of alpine lake ecosystems to even minor changes in water chemistry or nutrient availability.

The research reported herein was designed to investigate potential ecosystem impacts of eutrophication and trout introductions by examining the role of microbes in the structure and function of Sierran lakes. In oligotrophic aquatic ecosystems, including most alpine lakes worldwide, the microbial food web (bacteria and their protozoan grazers) is predicted to dominate the metabolism of carbon, nitrogen, and phosphorus. Without an understanding of the fundamental microbial processes and community structure in high-elevation lakes of the Sierra Nevada, the effects of eutrophication and introduced species on ecosystem processes are not predictable. Linking changes in lake community structure with changes in ecosystem function has received much attention in the recent ecological literature, but the majority of the research has been conducted in low-elevation, temperate lakes emphasizing predominantly “classical” food webs (phytoplankton to zooplankton to fish). This project extends that research into low-productivity ecosystems by focusing on the links between the structure and activity of the microbial food web and the ways in which microbes regulate organic matter cycling in high-elevation systems. The results of this research provide a thorough characterization of microbial communities in high-elevation lakes, a comprehensive analysis of interannual variation in community structure and metabolism, and experimental and observational data on the impacts of increased nutrients and introduced salmonids on the natural bacterial community.

Objectives

This research was designed to characterize the community composition and biogeochemical role of bacteria in high-elevation lake ecosystems of the Sierra Nevada. In addition, experimental and observational approaches were used to determine the impact of nutrient enrichment and introduced salmonids on the microbial community. Specific objectives of this work included:

- Develop a baseline description of the community composition of pelagic bacteria in high-elevation aquatic ecosystems of the Sierra Nevada.
- Determine the relative importance of bacteria in ecosystem metabolism of high-elevation lakes in the Sierra Nevada.
- Experimentally define the effect of nutrient enrichment on the community structure and metabolism of high-elevation bacterioplankton communities in a representative Sierra Nevada Lake.
- Analyze the environmental context of spatial and temporal variability in bacterial community structure throughout the Sierra Nevada, including seasonal phenology, landscape biogeography, and biogeochemical drivers.
- Examine the impact of introduced salmonids on the community structure of bacteria in high-elevation lakes of the Sierra Nevada.

Outline of Approaches

This multi-year study developed three datasets spanning both observational and experimental approaches at a range of spatial and temporal scales:

1) A three-year (2004-2006) study of bacterial metabolism, community structure, and biogeochemical processes throughout the water column of Emerald Lake, a representative high-elevation lake situated at 2800 meters above sea level in Sequoia National Park. The hydrology, biogeochemistry, and biology of the lake have been studied for more than 30 years, providing a rich contextual background for examining linkages between biogeochemistry, microbial dynamics, and lake metabolism.
2) An *in situ* experimental study examined the response of microbial communities to projected levels of atmospheric nitrogen and phosphorus depositional enrichment using microcosms over a period of several weeks in the summer of 2005.
3) A survey of over 100 lakes in fifteen catchments throughout the Sierra Nevada was used to characterize biogeographic variability of bacterial communities and to test whether community structure differed in lakes with and without introduced salmonids.

Methods

Study Designs

Characterization of Emerald Lake

The temporal and experimental components of the research detailed here were conducted at Emerald Lake, a headwater cirque lake located within Sequoia National Park on the western slope of the south-central Sierra Nevada (California, USA, 36°35'49"N, 118°40'30"W). The lake, situated at 2800 m above sea level in a sparsely forested granitic catchment, is representative of the > 4000 high-elevation (>2500 m a.s.l.) lakes scattered throughout the Sierra Nevada both in size (2.7 ha, 10.5 m z_{max}), solute chemistry, and catchment composition (Melack and Stoddard 1991). The lake has been studied for three decades, and its hydrology, biogeochemistry, and ecology are well-characterized (Melack et al. 1989; Sickman et al. 2003b). Emerald Lake is remote, accessible only by an 8 km hike (with nearly 2 km elevation gain) from the nearest road and 10 h from proper laboratory facilities. The lake has a single main inlet and several smaller inlets all of which consist of terrestrial runoff. Emerald Lake is dimictic and typically snow-covered November to June, with the timing of ice-off ranging from mid-May to late-July depending on the size of the snowpack and the timing of spring thaw. Spring mixing is brief, lasting about a week following ice-off, while fall mixing may continue sporadically for up to two months. Hypolimnetic temperatures range from 4 to 15 °C and epilimnetic temperatures can reach 22 °C. During summer stratification the primary thermocline is generally between 4 and 7 meters depth. Snowmelt flushing of nitrate is characteristic of catchments in the Sierra Nevada (Sickman et al. 2003a), such that concentrations within Emerald Lake range over an order of magnitude throughout the growing season as snowmelt progresses.

The lake was sampled approximately biweekly throughout the ice-free periods of 2004 and 2005 and three times in 2006. In addition, several samples were collected midwinter 2004 to 2005 and during the ice-covered snowmelt period in 2005 and 2006. All samples were collected and processed as described below. At each sampling timepoint vertical profiles of dissolved oxygen and temperature were conducted at 50 cm intervals with an elevation-calibrated, battery-operated, handheld meter (YSI 55). Magnitude and temperature of discharge from the lake were monitored continuously using a calibrated weir and pressure transducer with temperature sensor, and theoretical hydraulic residence time on each day was calculated as the number of summed preceding discharge days (m^3 d^{-1}) required to equal the lake volume (1.8×10^5 m^3). Lake thermal stability was calculated from thermal profiles according to Schmidt (1928) following the modifications of Idso (1973).

Survey of Sierra Nevada lakes

A survey approach was used to quantify variability in bacterial community composition among high-elevation lakes in the Sierra Nevada and to test for effects of introduced salmonids on bacterial community composition. Catchments

where lakes were surveyed are summarized in Table 1 below. Lakes in the Humphries Basin were sampled from the epilimnion via float tube as for Emerald Lake over a three-day period midsummer of each year 2004-2006. Lakes in the Tokopah Tablelands were sampled from the outflow over a 1-day period midsummer in 2005 and 2006. In the summer of 2006 (July to September) water samples were collected from 17 lake chains in 14 catchments throughout the Sierra Nevada. Sampling dates and relevant physical characteristics are listed in Table 1 below. Samples were collected at the outlet of each lake in a chain, and water bodies with surface areas < 0.5 ha were not sampled. ArcGIS (Environmental System Research Institute, Inc., Redlands, California, USA) was used to conduct all spatial analysis. Lake areas and flow path distances were measured using USGS topographic maps downloaded from the California Spatial Information Library (http://gis.ca.gov/). Catchment delineations and calculations of slope were based on 10 m digital elevation models downloaded from USGS National Elevation Dataset (http://seamless.usgs.gov/). Land cover characterizations were calculated based on USGS 2001 National Land Cover Database layers with 30 m pixel resolution (http://landcover.usgs.gov/). Each lake in a lake chain was assigned a Lake Network Number (LNN) based on the guidelines of Soranno et al.(1999). Lakes were assigned a LNN of 1 (hereafter referred to as primary or headwater lakes) if there were no upstream lakes with surface areas > 0.5 ha. Data for salmonid presence and density (calculated as catch per unit effort during gill-net surveys) were acquired from Dr. Roland Knapp at the University of California Natural Reserve System Sierra Nevada Aquatic Research Laboratory and from the California Department of Fish and Game according to the methods outlined by Knapp and Matthews (2000).

Nutrient Enrichment Experiment

Two separate *in situ* carboy experiments were conducted for 8-12 days each in Emerald Lake during the summer of 2005 to contrast impacts of nutrient enrichment on heterotrophic prokaryotes with impacts on the microbial community as a whole. Both experiments consisted of nine experimental units divided into three treatments replicated in triplicate: treatment (P) was enriched with K_2HPO_4, treatment (N) was enriched with KNO_3, and treatment (Control) was enriched with a comparable volume of distilled water and served as a control. Final nutrient concentration enrichment targets of 2 μmol L^{-1} phosphate and 10 μmol L^{-1} nitrate in the enriched carboys were selected in accordance with previous enrichment experiments conducted in the region (Sickman 2001) for the sake of maximizing historical comparability. Carboys were collapsible plastic 'cubitainers' which had been leached in 10% HCl for three days, rinsed, dried, then leached again for several hours with water from Emerald Lake just prior to deployment. Carboys were deployed at 2 m depth in the center of Emerald Lake and were removed every few days for 2-3 hours for periodic sampling.

The first experiment (DARK) was conducted using 10 L cubitainer carboys constructed of opaque, black, low density polyethylene (LDPE; Reliance Products 932163) wrapped in mylar to minimize heat absorbance. Lakewater was collected from the center of Emerald Lake at 0.5 m depth and each carboy was promptly filled with 7.5 L of dilution culture: 2.5 L of whole lakewater diluted with 5 L

lakewater filtrate which had been gravity-filtered through a nitrocellulose filter (GE/Osmonics E02WP14225, 142 mm diameter, 0.22 μm pore-size). Before collecting filtrate, each filter was flushed with 350 mL lakewater to extract filter-derived contaminant organics, and filters were typically changed after filtering 3 to 4 L lakewater. Due to logistical constraints, dilution cultures could not be initially homogenized between carboys, and as such each carboy is analyzed using a separate starting point sample collected within 1 hour of mixing, although there were no significant differences between treatments at the start of the experiment in any of the measured response variables (ANOVA, $p > 0.15$). Once all dilution cultures had been prepared (a process which took approximately 6 h), carboys were amended with nutrients according to treatment categories, sampled, and deployed in the lake.

The second experiment (LIGHT) was conducted using 10 L carboys constructed of transparent LDPE (Reliance Products 250013) filled with 7.5 L whole lakewater collected from the center of Emerald Lake at 0.5 m depth and promptly amended with nutrients as described above. Because lakewater used in this experiment was unadulterated and homogenous between carboys, initial sampling was restricted to one carboy from each treatment for determination of variance in initial conditions, and statistical analyses excluded the initial timepoint.

The experiments detailed herein were conducted from July to September of 2005, a water-year marked by near-record winter snowpack duration. The ice cover on the lake melted in mid-July, such that the summer growing season serving as the backdrop to these experiments was relatively short (Tonnessen 1991). The DARK experiment was conducted for one week 27 July - 2 August, 2005 when the lake was characterized by rapid flushing (residence time 20 d), post-snowmelt stratification (T_{surf} 14.2 °C, T_{8m} 8.0 °C, thermal stability 32 kJ m^{-2}), and low chlorophyll a concentrations (0.47 μg L^{-1}). The LIGHT experiment was conducted for twelve days 18 to 30 September, 2005 when the lake was characterized by longer theoretical hydraulic residence time (250 d), post-stratification mixing (T_{surf} 14.9 °C, T_{9m} 13.3 °C, thermal stability 6 kJ m^{-2}), and increased chlorophyll a concentrations (0.84 μg L^{-1}).

At each sampling time (every one to three days, see Figs. 16-19), carboys were removed from the lake for 2-3 hours for processing. Samples collected and parameters measured included the following: particulate carbon, nitrogen, and phosphorus (PC, PN, PP); total dissolved nitrogen and phosphorus (TDN,TDP); dissolved organic carbon (DOC); dissolved inorganic nitrate/nitrite (DIN); dissolved soluble reactive phosphorus (SRP); prokaryotic abundance; DNA. In addition, LIGHT carboys were sampled for particulate chlorophyll a and prokaryotic production. All parameters were measured at each time from each carboy, such that each sampling event reduced carboy volume by roughly 1800 mL (with the exception of days 8 and 13, wherein only 400 mL were removed and only DOC, prokaryotic abundance, and DNA were sampled).

Repeated measures multivariate analysis of variance (RM-MANOVA) was used to test the null hypothesis of no difference between nutrient-enriched and control treatments across sampling times for a suite of response variables. The repeated-measures design accounts for within-carboy correlation through time and the multivariate approach avoids Type I errors caused by violations of the assumption of sphericity associated with univariate ANOVA in repeated-measures designs

(O'brien and Kaiser 1985). Triplicate carboys were grouped according to treatment within each time and separate analyses were conducted for each response variable comparing each nutrient with the control. Response variables included all measured and calculated chemical analyses, prokaryotic abundance and production, and relative abundances of each unique phylotype. In order to ascribe terminal restriction fragment length polymorphisms (TRFLPs; a measure of bacterial community composition, see below) to specific bacterial phylotypes clone libraries were constructed from environmental samples drawn from the lake within days of the start of each experiment (31 July 2005 and 18 September 2005) and phylotypes were ascribed to TRFLP data as described below.

Catchment Name	Sampling Dates	Lat. UTM Z11 North (m)	Long. UTM Z11 East (m)	Avg. Elev. (m)	# of lakes	#fish-less lakes
Dicks Lake #	7/4-6/2006	4313539	227455	2409	7	0
Boundary Lakes	7/1-2/2006	4216880	254589	2187	9	7
Ten Lakes	7/18/2006	4197620	277876	2790	4	0
Virginia Lakes #	7/19/2006	4213532	300570	3077	7	1
Lundy Canyon #	9/8/2006	4208961	299518	2857	6	0
Shadow Lakes #	7/20-1/2006	4173066	309976	2849	5	0
Little Lakes	7/22-4/2006	4141196	344296	3311	14	1
Steelhead Lakes	8/25/2006	4129073	347269	3405	5	0
Puppet Lakes	8/26/2006	4127432	345091	3409	4	0
Evolution Valley	8/16-7/2006	4111583	349760	3401	7	2
Rae Lakes	9/5/2006	4075398	374747	3192	7	0
Sixty Lakes	9/6/2006	4075838	373047	3273	10	1
Forester Pass	8/8-9/2006	4060544	376804	3732	6	5
Cottonwood Lakes #	8/28/2006	4039621	390807	3383	5	0
Humphries Basin*	2004-2006	4125670	347852	3365	8	4**
Tokopah Tablelands*	2005-2006	4052486	351814	3102	11	7

Table 1. **Summary of characteristics of lakes sampled in survey work.** *Lakes in Humphries Basin were sampled 7/04, 9/05, 8/06. Lakes in the Tokopah Tablelands were sampled 8/05, 8/06. **The four fishless lakes in the Humphries Basin were previously stocked and had all fished removed via gill-netting prior to this research as follows: Knob Lake 1998-2000, Square Lake 1998, Marmot Lake 1998-2000, Coney Lake 2000-2002. All CPUE data from Dr. Roland Knapp at UCSB-SNARL except # from CDFG.

General Laboratory and Field Measurements

Sample Collection and Storage

At each measurement time ~6 L water for chemical analyses was collected via hand-cranked peristaltic pump through siliconized polyethylene tubing into collapsible 10 L low-density polyethylene carboys (Reliance Products 250013). For surveys in 2006, samples were hand-collected in slow-flowing water at lake outlets. Samples collected and parameters measured included the following: particulate carbon, nitrogen, and phosphorus (PC, PN, PP); total dissolved nitrogen and phosphorus (TDN,TDP); dissolved organic carbon (DOC); dissolved inorganic nitrate/nitrite (DIN); dissolved soluble reactive phosphorus (SRP); and chlorophyll a concentration. An additional water sample from each location was pumped directly into polycarbonate bottles for collection of DNA for bacterial community analysis to avoid alteration of community structure by extended contact with polyethylene leachates. All plasticware was acid-washed and rinsed between sampling events and triple-rinsed with sample water before collection.

Particulates were collected by gentle gravity filtration of ~450 mL sample water onto combusted (2 h at 450 °C) 47 mm Whatman GF/F filters (nominal pore size 0.7 μm) held in polycarbonate in-line filters. One filter was used for chlorophyll analysis, a second for PC and PN, and a third for PP, each folded closed, wrapped in aluminum foil, and frozen (-20 °C) upon return to the laboratory. Dissolved nutrients (TDN,TDP,DIN,SRP) were analyzed from GF/F filtrate collected in new, rinsed HDPE bottles (Nalgene). DOC and dissolved fluorescence were analyzed from GF/F filtrate collected in acid-washed, combusted (12 h at 450 °C), amber glass EPA vials (I-Chem) with siliconized septa immediately amended with acid (to ~20 μM HCl) and stored frozen (-20 °C) upon return to the laboratory. DNA samples were collected from polycarbonate bottles by filtration of ~400 mL whole water sample onto a 0.22 μm polyethersulfone filter cartridge (Millipore Sterivex SVGP01050) which was immediately emptied of water, filled with sucrose lysis buffer (40 mmol L^{-1} EDTA, 50 mmol L^{-1} Tris-HCL, 750 mmol L^{-1} sucrose, pH adjusted to 8.0), sealed with parafilm, and stored frozen (-80 °C) on return to the laboratory.

Chemical analytical procedures

PC and PN were analyzed via double-drop GF/F combustion on an organic elemental analyzer (Control Equipment Corporation Model 440HA) by the UCSB Marine Science Institute Analytical Lab. Particulate Chlorophyll a was analyzed by dark-digesting filters 24 to 48 h in 90% acetone at -20 °C followed by 10 min dark centrifugation and immediate fluorescence analysis on a Turner AU-10 fluorometer (Smith et al. 1981). DIN and SRP were measured by the UCSB Marine Science Institute Analytical Laboratory on a Lachat Instruments Quickchem 8000. TDN and TDP were measured as DIN and SRP from an identical sample analyzed following digestion [10 mL sample amended with oxidation reagent and autoclaved according to Valderrama (1981)], neutralization with NaOH, and subtraction of digested double-distilled H_2O blanks. PP was analyzed by digesting GF/F filters in 30 ml ddH_2O amended as for TDN/P above

and measuring SRP after filter-blank subtraction to correct for silicate interference. DON was calculated as the difference between TDN and DIN and TP was calculated as the sum of PP and TDP. DOC was analyzed on a Shimadzu TOC-V adapted to increase precision below 100 μM [detailed in Carlson et al. (1998)].

Bacterial abundance and rates of cellular production

Samples for bacterial production consisted of 30 mL whole water collected in acid-washed triple-rinsed polycarbonate centrifuge tubes (Oakridge) with polyethylene lids just before departure from the field site and were analyzed immediately upon return to the laboratory. Bacterial production (BP) was measured by incubating 1.7 mL whole water samples with 20 nmol L^{-1} L-[4,5-^{3}H] Leucine (Amersham TRK636, 63 Ci $mmol^{-1}$) for 90 to 120 minutes. Samples were processed and analyzed according to Smith and Azam (1992). Bacterial abundance (BA) was analyzed from 10 mL whole-water samples immediately amended to 2% formalin and refrigerated up to 3 days upon return to the laboratory. Abundance was determined by epifluorescence microscopy of formalin-preserved specimens stained with the nucleic-acid fluor DAPI [4',6'-diamidino-2-phenylindole, Porter and Feig (1980)]. Between 2 and 6 mL of formalin-preserved water was filtered onto a 0.22 μm polycarbonate filter stained with irgalan black (to enhance contrast) and then incubated 5 min in 5 mg mL^{-1} DAPI. Abundance was determined as the average of 10 fields (volumes filtered generally yielded 30-300 cells per field). Cell-specific bacterial production (SP) was calculated as the ratio of BP to BA (zmol ^{3}H-Leu L^{-1} h^{-1}). Ratios of bacterial organic carbon to non-bacterial particulate organic carbon (BOC:POC) were calculated by converting BA to carbon units as above and adjusting values for the fact that 60% of both BA and BP are captured in the particulate fraction (BA and BP in GF/F filtrate consistently decline to 40% of whole water values; data not shown).

Microbial community metabolic rates

Net primary production (NPP) and bacterial growth efficiency (BGE) were measured on a subset of sampling dates using water collected from 2 m and 8 m depth. NPP was measured via the ^{13}C method (Hama et al. 1983) using 24 h in situ incubations to estimate net rates of photosynthetic production because of restrictions on radioisotope use in wilderness jurisdictions of the United States. Briefly, whole water was placed into five identical 0.5 L polycarbonate bottles (to maximize transparency to photosynthetically active radiation) and amended with $H_2{}^{13}CO_3$ to a final concentration of 5-10% of dissolved inorganic carbon. One bottle was filtered 20 minutes after amendment to determine initial $\delta^{13}C$ and duplicate bottles were incubated at 2 m and 8 m and filtered after 24 h to determine final $\delta^{13}C$. Dissolved inorganic carbon concentration was calculated from measured alkalinity, pH, temperature, and conductivity (Kling et al. 1992) and rates of NPP were calculated as net relative increase in $P\delta^{13}C$ (Hama et al. 1983).

BGE was measured only in 2005 via dilution culture (Del Giorgio and Cole 1998). Water was collected from 2 m and 8 m depth in 500 mL polycarbonate bottles (to minimize leaching of phthalates associated with polyethylene) and 70% of the volume was filtered through a sterile 0.22 μm polyethersulfone filter cartridge (Millipore Sterivex SVGP01050) following a 50 mL flush to remove exogenous DOM from the filter. The remaining whole water was used to inoculate the filtrate and the bottles were incubated in the dark at in situ temperatures for 5-7 days. Bottles were sampled daily for DOC concentration and prokaryotic abundance as detailed above. BGE was calculated as the slope of a regression comparing decline in DOC to increase in cellular carbon [and discussed in Ducklow (2000); assuming 20 fg C $cell^{-1}$, Lee and Fuhrman (1987)]. All regressions were highly significant ($p < 0.001$) with average $r^2 = 0.71$. Bacterial respiration rates were calculated as the rate of BP [converted to carbon units as 1.5 kg C mol^{-1} Leu; (Simon and Azam 1989)] subtracted from the rate of bacterial carbon demand, calculated as the measured ratio of BP:BGE (Del Giorgio and Cole 1998).

Bacterial community fingerprinting

Terminal restriction fragment length polymorphism (TRFLP) was used as a fingerprinting method for comparison of bacterial community composition between DNA samples (Liu et al. 1997). Sterivex capsules were thawed and amended with proteinase K (0.2 mg mL^{-1}) and lysozyme (0.5 mg mL^{-1}) at 37°C for 30 minutes followed by 55°C for 2 to 12 hours and extracted immediately. Genomic DNA extraction was done using Qiagen DNEasy centrifuge columns. Extracted DNA was amplified by polymerase chain reaction (PCR) as follows: a reaction mix consisting of 2.5 mmol L^{-1} $MgCl_2$, 200 μmol L^{-1} dNTP mix, 5% Acetamide, 4 to 14% template (~ 10 ng), 10 μL mineral oil, 1 unit *Taq* DNA Polymerase in buffer, and 200 nmol L^{-1} each of primers 27F (AGAGTTTGATCMTGGCT, FAM-labeled) and 519R (GWATTACCGCGGCKGCTG, unlabeled) was subjected to thermocycling consisting of 3 min initial denaturation at 94 °C, 30 cycles of 1 min 94 °C denaturation followed by 1 min 58 °C annealing followed by 2 min 72 °C extension, and 10 min final extension at 72 °C before being held at 4 °C until further processing. PCR products were cleansed of small fragment DNA using the Qiagen QiaQuick DNA Cleanup Kit and then digested 4 hours at 37 °C with restriction enzyme HaeIII (New England Biolabs, 5% final concentration) followed by 20 min at 80 °C for enzyme inactivation and stored at 4 °C.

Digest products were analyzed on an Applied Biosystems ABI 310 sequencer using Genescan Software. A size standard (MapMarker 1000) was run with every sample to define the standard curve between 25 and 600 base pairs (bp), and the Global Southern curve-fitting algorithm was used to calculate bp lengths of identified fluorescence peaks. The peak idenfication cutoff for relative fluorescence units (rfu) was typically 50 rfu, minimum peak half-width was 3 data points, and the typical range of quantified peaks was 300 to 3000 rfu. Samples were completely re-processed if the bulk of the peaks in the electropherogram were below 500 rfu. TRFLP data from all samples were aligned using a novel frequency-based alignment method. Briefly, all TRFLP electropherograms

generated from this study were pooled and peaks were sorted by length. Fragments within length ranges where multiple samples exhibit dominant electrophoretic fluorescence peaks were assigned integer lengths based on the mean and variance of each group and the size of the gap between regions of higher sample density. This method avoids the inaccuracies associated with common approaches to "binning" fragment lengths using integer rounding or truncation methods [see also Hewson and Fuhrman (2006)].

Bacterial community composition data for all samples were collated using relative abundance data [estimated as within-sample relativized eletropherogram peak area for each fragment (Yannarell and Triplett 2005)] after removal of fragments which appeared only once in the entire dataset and all fragments less than 150 bp (due to size-calling algorithm inaccuracies). Multivariate community distances were calculated as the Sørenson dissimilarity index [aka Bray-Curtis or Percent Dissimilarity, calculated 1-2W/(A+B) where W is the sum of shared relative abundances and A and B are the sums of relative abundances in individual sample units; (Sørensen 1948)] using PC-ORD software (Mccune and Mefford 2006). Samples were clustered (Fig. 7) using the Flexible-β algorithm (β = -0.25) in PC-ORD and divided into groups using a distance cutoff selected in order to minimize number of groups, minimize within-group distances, and maximize variance explained (estimated using the "elbow criteria" in a graph relating variance explained to number of groups). Nonmetric multidimensional scaling (NMS) was employed to ordinate data in a lower-dimensional space (Fig. 9), and the multiresponse permutation procedure (MRPP) was implemented in PC-ORD to test the null hypothesis of no difference in bacterial community composition between sampling dates and/or treatments. Sample phylotype richness and the Shannon diversity index were also calculated from relative abundance data derived from TRFLP fingerprint analysis.

Phylogenetic identification of bacterial taxa

In order to ascribe terminal restriction fragment lengths to specific bacterial phylotypes five clone libraries (96 attempted clones in each) were constructed from environmental samples drawn from the lake in 2005. Libraries were generated from 2 m depth samples on three dates (6/6/05, 7/31/05, and 9/18/05) to capture the three interannually recurring TRFLP community types (Figs. 8-10) and one library was generated from the inlet on 6/6/05. DNA from these environmental samples was extracted using identical methods as above and duplicate 100 µL PCR reactions were carried out as above except without a FAM-tag on the 27F primer. PCR products were concentrated twofold using QiaQuick columns, then gel-extracted and further concentrated to 30 µL with a second QiaQuick column. PCR products were then ligated into the pGEM-t plasmid cloning vector (Promega) and transformed into competent E. coli DH5α according to vendor guidelines. Transformants were plated onto LB/Amp (100 µg ml^{-1})/X-Gal/IPTG plates, randomly selected for sequencing via white/blue screening, and sequenced via unidirectional rolling-circle PCR by the University of Washington High Throughput Sequencing Facility.

Sequences were collated and trimmed to the primer region using the BioEdit program (Hall 1999), aligned using the NAST aligner (Desantis et al. 2006a),

classified using maximum likelihood algorithms to the GreenGenes 16S rDNA database (Desantis et al. 2006b) and checked for chimeras using Bellerophon 1.3 (Huber et al. 2004). Putative chimeras and sequences classified as plastids were excluded from further analyses, the library was dereplicated into unique phylotypes using FASTGROUPII (Yu et al. 2006) at a level of 97 percent sequence identity, and the remaining sequences were digested in silico using the Sequence Manipulation Suite software (Stothard 2000).

A subset of 25 clones representing unique in silico restriction lengths were analyzed via TRFLP (as above except plasmid DNA was extracted using Qiagen Miniprep columns rather than DNEasy) using the duplicate pooling approach detailed by Grant and Ogilvie (Grant and Ogilvie 2004). A linear regression ([GeneScan bp length] = 1.018 [in silico bp length] - 7.583; r^2=0.9999; range 39-517 bp) was used to correct Genescan-estimated TRF lengths from experimental samples and representative clones were ascribed to each matching TRF length (Brown et al. 2005; Morris et al. 2005; Stepanauskas et al. 2003).

A phylogenetic tree was constructed from the pooled clone library sequences in order to analyze phylogenetic structure of bacterioplankton across seasons (Fig. 11). Aligned sequences of 3 the three most similar cultured and uncultured sequences to each Emerald Lake clone and in the GreenGenes prokMSA database (along with a single Archeal outgroup sequence) were combined into a complete alignment (800 sequences altogether, 351 clones and 449 GenBank/prokMSA sequences) to ensure accurate tree construction. The software package PHYLIP (Felsenstein 2005) was used to generate a neighbor-joining tree from a distance matrix of the aligned sequences (using the DNADist and NEIGHBOR algorithms). The resulting tree was then uploaded to the Interactive Tree of Life (Letunic and Bork 2007) and pruned to remove sequences not derived from this study. Nodes were assigned taxonomic identities when possible based on lowest defined classification level of the sequences within a cluster displaying maximum likelihood similarity of > 0.85 to classified prokMSA sequences (Hugenholtz taxonomy). The distribution of nodes among environments were calculated as follows: within-sample clone count from a given node was divided by the total number of unique clones for a given environment to generate relative within-sample abundance (e.g. 5% of 6/6/05 inlet clones are α-proteobacteria) then this value was divided by the total relative abundance for the node to generate pie charts (e.g. α-proteobacteria were a larger fraction of 6/6/2005 lake clones than 7/31/05 lake clones; Fig. 11).

Results

Role of bacteria in metabolism of Emerald Lake

Interannual variability of lake physicochemical properties

The sampling period 2004-2006 spanned a wide range of regional climate patterns, with 2004 a relatively dry year and both 2005 and 2006 exhibiting near-record winter precipitation and snowpack duration. These large-scale climate patterns led to distinct differences in the physical and biological characteristics of the lake between years (Figs. 1-4, 8). Peak snowmelt discharge in 2004 was < 10,000 m^3 d^{-1}, snowmelt extended from late April to mid-June, and the ice cover on the lake melted in late-May. In contrast, 2005 and 2006 both exhibited peak discharge values > 40,000 m^3 d^{-1}, with snowmelt extending from mid-May to late August and the lake remaining fully ice-covered until mid-July. The duration and magnitude of summer stratification were larger in 2004 than in 2005 and 2006, and the length of the growing season was considerably curtailed in the latter years due to early (20 d earlier) onset of fall overturn. Average integrated stocks of both dissolved and particulate organic carbon in 2004 were nearly double those of 2005 and 2006, and similar trends were observed in rates of primary production and concentrations of chlorophyll a (data not shown). Average water-column nitrate concentrations were higher in 2005 than 2004 or 2006 and all three years saw the characteristic steady decline in lake nitrate concentrations with declining snowmelt inputs (Fig. 8). Residence times of the lake during the sampling period ranged from 40 – 170 d in 2004 and 4 – 80 d in 2005 and 2006 (Figs 1,8). Maximum surface water temperatures in 2004 were 21 °C and in 2005-6 were 18 °C, and lake thermal stability ranged from 0.06 to 42 kJ m^{-2} in all years (Fig. 8).

Biogeochemical dynamics

Emerald Lake exhibited consistent increases in productivity throughout the ice-free periods of both 2004 and 2005 (Fig. 2), with productivity patterns generally tracking physical processes within the lake (Figs. 1, 2). Patterns in productivity were consistent across a range of measurements, with strong relationships between primary productivity (chlorophyll and NPP, Fig. 2) and organic matter composition (DOC:PC; Figs. 2,3). Chlorophyll *a* concentrations ranged from 0.01 to 4 μg L^{-1} across the dataset and displayed higher mean concentrations in 2004 (0.98) than in 2005 (0.68), with levels generally increasing throughout the growing season and consistently highest following fall overturn. Particulate carbon concentrations were roughly three times higher in 2004 (10-60 μmol L^{-1}) than in 2005 (3-22 μmol L^{-1}; Fig. 2) and were proportional to chlorophyll concentrations across years ($r^2 = 0.64$, $p < 0.001$, $n = 58$). Rates of NPP were weakly corellated with chlorophyll concentrations across both years ($r = 0.53$, $p = 0.007$, $n = 24$) and ranged from 0.6 to 44 μg C L^{-1} d^{-1} (Figs. 2,4). Dissolved oxygen was generally 80 - 100% saturated and ranged from 6 - 10 mg L^{-1} during the ice-free period (shifting to hypoxia ~4 mg L^{-1} in the hypolimnion during the icebound winter period; Fig. 1). A transient increase in productivity was observed in both years at 8 m depth during peak stratification, suggesting a deep-water

bloom and resulting in an increase in dissolved oxygen at depth. A large proportion of total variability in both chlorophyll and PC was described by lake residence time (r^2 = 0.60 and 0.42 respectively, $p < 0.001$, n = 58), which captured interannual variability in the timing of limnetic transitions.

Dissolved organic matter ranged from 1 to 20 times particulate organic matter concentrations (average ~3) and this ratio decreased throughout the growing season with a maximum during peak snowmelt (Fig. 2). DOC:PC was marginally higher in 2005 than 2004 but DON:PN in 2004 was nearly double 2005 values. DOC and DON concentrations were typically twice as high in 2004 than in 2005, with average 2004 concentrations of 76 and 17 μmol L^{-1}, respectively, and average 2005 concentrations of 47 and 2.7 μmol L^{-1}, respectively (Fig. 2). DOC:PC ratios were inversely proportional to chlorophyll concentrations across both years (r^2 = 0.58, $p < 0.001$, n = 58).

Bacterioplankton dynamics

Bacterial abundance ranged over nearly two orders of magnitude from 1.6 X 10^8 to 6.3 X 10^9 cells L^{-1} and averaged 1 X 10^9 in both years (Figure 3). Cell concentration increased throughout the season, with hypolimnetic peaks during the stratified period in both years 2-4 weeks following peaks in primary productivity and increasing trends following fall overturn. The ratio of bacterial carbon to non-bacterial particulate carbon (BOC:POC) ranged from 1 to 300% and averaged 40% across years (Fig. 3). Bacterial abundance was significantly related to chlorophyll concentrations across years and depths (Fig. 5) and chlorophyll-specific bacterial abundance (BA:Chl) declined with increasing chlorophyll (r^2 = 0.69, $p < 0.001$, n = 58). Bacterial production ranged from 2 to 184 pmol ^{3}H-Leu L^{-1} h^{-1} and was variable throughout the water column and through time (Fig. 3), with average rates higher in 2004 than in 2005 (76 and 33 respectively). Cell-specific growth rates (SP) were also variable, with highest values under the ice in 2005 and midsummer 2004 and generally low during the growing season of 2005 (Fig. 3). Bacterial production was not significantly related to chlorophyll concentration (Fig. 7) or BGE (data not shown) but chlorophyll-specific BP declined with increasing productivity (r^2 = 0.62, $p < 0.001$, n = 58).

Bacterial growth efficiency displayed a wide range of values across the data set, (0.16 to 0.61) and was relatively high for an oligotrophic pelagic system (mean 0.38; Fig. 4). This temporal variability matches the range of values found throughout the literature across a range of ecosystem trophic types (Del Giorgio and Cole 1998). BGE was significantly predicted by chlorophyll (Fig. 7) and NPP (Fig. 8), with efficiencies increasing with increased phytoplankton production. BGE was not significantly related to BP ($p > 0.1$, n = 13), and consequently rates of bacterial respiration were negatively related to BGE (r^2 = 0.62, $p < 0.01$, n = 13, data not shown). BR therefore was inversely proportional to chlorophyll and NPP and increased with increasing bacterial production (Figs. 7,8). Rates of bacterial respiration ranged from 0.3 to 16 μg C L^{-1} d^{-1} (Fig. 5) and chlorophyll-specific BR declined with increasing productivity (r^2 = 0.91, $p < 0.001$, n = 13). The ratio BR:NPP serves as an estimate of ecosystem metabolic balance (Del Giorgio et al. 1997), and this ratio ranged from 0.02 to 1 within 2005 and declined

throughout the growing season (Fig. 4). BP:NPP ranged from 0.003 to 5.4 (Fig. 4), but average values fell in the range previously reported across pelagic ecosystems [0.1 – 0.3, (Cole et al. 1988; Ducklow 2000)]. Although BGE (and thus BR) was not measured in 2004, BR:NPP is coupled to BP:NPP (Cole 1999) and was highly predictable from BP:NPP within 2005 ($r^2 = 0.84$, $p < 0.001$, $n = 9$). Using this model to estimate BR:NPP in 2004 (Fig. 4), when ratios of BP:NPP were significantly higher, indicated that BR:NPP ranged from 0.05 to > 16, suggesting the system was net heterotrophic in the early season. Both BR:NPP and BP:NPP were negatively related to BGE and NPP ($r^2 = 0.63$ and 0.61 respectively, $p < 0.01$, $n = 9$ and 24, Fig. 8), indicating that increases in productivity shifted the system seasonally to net autotrophy.

Phenology of bacterioplankton

Patterns in community fingerprints

Multivariate clustering of TRFLP samples (Fig. 7) based on relative fragment fluorescence revealed a variety of temporal and spatial patterns in bacterial community composition. Seven distinct community types were delineated within the data (see Methods), with groupings determined to be significantly different using the multi-response permutation procedure in PC-ORD (MRPP; $A = 0.28$, all pairwise and pooled $p << 0.001$, within-group dissimilarity < 50% except inlets = 0.62). MRPP results were nearly identical when the TRFLP fragment distance matrix was converted to presence-absence, indicating that community types differed in both taxonomic composition as well as relative taxa abundances. Inflowing terrestrial runoff communities were distinct from lake communities across all three years and were markedly dissimilar to each other, but were generally more similar to lake communities during snowmelt periods than at other times of year (Fig 7). Communities were more similar within sampling dates than between dates (Figs. 7,8), although this trend was generally only true when the water column was well-mixed. In fact, community distance throughout the water column on a given date was positively related to both water-column distance and degree of stratification (Fig. 10). During strongly stratified periods epilimnetic and hypolimnetic communities were sufficiently distinct to be grouped as separate community types, with hypolimnetic communities generally grouping with adjacent timepoints (Fig. 8).

Three lake community types were observed to recur each year while the remaining types were unique to a given year and emerged only during stratified periods (Figs. 7,8). Communities were most similar interannually during fall following overturn (Fall Overturn Group). Lake communities during peak snowmelt periods (before ice-off) were similar in 2005 and 2006 (Snowmelt Group; this period was not sampled in 2004) as were lake communities found during early stratification following ice-off in 2004 and 2005 (Ice-Off Group; this period was not sampled in 2006). Lake community types were significantly different with respect to ordinal date, residence time, and thermal stability (ANOVA $p < 0.0001$) and discriminant analysis using residence time and thermal stability alone successfully delineated community type for >75% of samples, with a model incorporating ordinal date delineating 87% (stratified samples were

poorly discriminated among years by these physical variables alone and were excluded from this analysis).

Community fingerprint relative abundance data were ordinated via NMS into two dimensions (final stress = 18.7, cumulative r^2 between ordination distances and original distances = 0.77, axes 99.2% orthogonal, inlet samples excluded n = 80, Fig. 9). Lake thermal stability and residence time displayed the strongest univariate regressions with the respective orthogonal NMS axes (r^2 = 0.51 and 0.67, $p << 0.01$; Fig. 9). In addition to these physical variables, temperature, nitrate, PC, PN, DOC, DON, and chlorophyll a were all significantly related to axes of community variability ($p < 0.01$), with coefficients of determination ranging from 0.15 to 0.27 (data not shown). Raw matrix correlations between TRFLP relative fluorescence data and environmental parameters conducted using the BIO-ENV algorithm supported the strong correlation between community structure and residence time (Mantel r = 0.64), with thermal stability, temperature, nitrate, and DON lending additional descriptive ability (r = 0.73 for a distance matrix generated from all five parameters).

Clone library analysis

Five separate clone libraries were generated from four unique DNA samples for a total of 351 non-plastid clone sequences. All but 15 of these clones (95.7%) displayed in silico restriction lengths which were represented in the TRFLP dataset, and 86.2% of the total TRFLP fragment relative peak area in the dataset was successfully matched to a representative clone (within ±0.5 bp of in silico length after correction; see Methods). Using a 97% sequence identity, the number of unique phylotypes in each library ranged from 25-56 (roughly matching TRFLP Richness of 26-33) and bootstrapped estimates of actual sample α-diversity (using the Chao1 metric) ranged from 62-125. Estimated coverage of diversity ranged from 32-50% but did not increase with library size, suggesting inadequate coverage of diversity, despite asymptotic behavior of sampling curves in several cases. Pooling libraries across lake samples produced a similar increase in both measured (99) and estimated (252) β-diversity with no concomitant increase in pooled coverage estimate (remained ~ 50%).

Dereplication of the library at the 97 percent sequence identity level yielded 118 unique taxa, 94 of which displayed unique NCBI TaxID codes based on maximum likelihood similarity to GenBank sequences. A pruned phylogenetic tree of these 94 representative sequences is displayed in Figure 11. In general, the bulk of clones were classified in the Actinobacteria, Bacteriodetes, and β-Proteobacteria. 70% of the sequences were unique, while 18% were found five times or more. The greatest diversity of clones was found in the β-Proteobacteria, with the Burkholderiales family alone containing 19 unique sequences and 82 total clones. The α- and γ-Proteobacteria were represented by 8 and 10 sequences, respectively, many of which were unique and only rarely found in the TRFLP dataset. In general, clades were unevenly represented among environments, with early-season samples dominated by Flavobacteria and β-Proteobacteria and late-season samples dominated by Actinobacteria and Sphingobacteria.

Temporal dynamics and environmental correlates of bacterial phylotypes

The temporal dynamics of dominant clades and representative fragments throughout the sampling period in 2004 and 2005 are shown in Figure 12. The proportion of total fragment abundance comprised of the 8 dominant clades (and also of their representative fragments) is generally higher during the growing season, while during midwinter and snowmelt periods evenness increases. Flavobacteria comprised a larger proportion of the community during periods of mixing (ice-off and fall overturn) and Actinobacteria became dominant during stratified periods. Burkholderiales were generally a large component of the community, with relative declines during periods of mixing. Verrucomicrobia were generally a small proportion of the community with modest peaks in relative abundance during periods of stratification. Cyanobacteria were a significant proportion of the community only after the onset of stratification, and their relative abundances generally tracked patterns of primary production in the lake. Sphingobacteria and Methylophilales were a significant proportion of the community in early-season community types during peak-snowmelt periods. The inlet community was dominated by Microbiaceae and β-proteobacteria.

Stepwise multiple regressions were used to determine the proportion of variability in relative abundances of dominant clades explained by various environmental factors (data not shown). Particulate organic measurements (PC, PN, chlorophyll concentrations) were infrequently included in the final models and were seldom significantly related to clade relative abundances. Coefficients of determination for the multivariate models ranged from 0.14 (Verrucomicrobia) to 0.84 (Methylophilales) with an average of 0.41. Residence time and thermal stability were significantly related to the relative contribution of every clade save the Burkholderiales and Cellulomonadceae, both of which were best described by nitrate concentrations and temperature. Temperature was also a significant predictor of the relative contribution of Sphingobacteria and Methylophilales. DOC was weakly but significantly related to Cyanobacterial relative contributions, and TP was the best descriptor for Flavobacteria.

Bacterioplankton biogeography and relationship to introduced salmonids

A significant positive relationship was found between lake flowpath distance and Sørensen distance for TRFLP data from lake outflows (Fig. 13b). A similar relationship was found between Sørensen distance and the degree of lake network separation (Fig. 13a). This line of evidence is one of the first examples of true biogeographic patterning in prokaryotic organisms. Demonstrating that increased physical separation along hydrologic flowpaths is significantly related to community differentiation lends support to the idea that isolation and dispersal are mechanisms driving community differentiation in microbial populations and communities.

No significant difference was found between TRFLP community fingerprint samples from lakes containing introduced salmonids and those which may be considered “fishless” (MRPP A = 0.005 for fish and fishless groupings, $p > 0.01$, within-group distances ~ 0.75, same result for definitions of “fishless” ranging from CPUE = 0 to CPUE < 2.5). NMS ordination of samples in a two-

dimensional space (Fig. 14, stress = 0.22) did not yield any significant correlates between axes of community structure and a suite of 28 biogeochemical and landscape-composition variables. However, fish presence and density were both significantly positively related to bacterial richness and biodiversity H' (Fig. 15). Forward stepwise multiple regression analysis of biogeochemical variables against bacterial richness revealed fish density as the strongest predictor (partial r^2 = 0.17, std. β = 0.41), with the final model r^2 = 0.40 and containing bulk catio concentration, SRP concentration, and DON concentration as additional regressors significant in the final model. There were no strong correlations (Pearsons $r < 0.3$) between any specific bacterial phylotype (n = 152) and salmonid density (CPUE).

Response to experimental nutrient enrichment

Biogeochemical response

Nutrient enrichment in the DARK experiment increased mean DIN levels from 4.2 μmol L^{-1} to 15.9 μmol L^{-1} and mean SRP levels from 0.04 μmol L^{-1} to 1.6 μmol L^{-1}, altering mean starting DIN:TP molar ratios to 2.7, 161, and 59 for P, N, and C treatments respectively. Nutrient enrichment in the LIGHT experiment increased mean DIN levels from 0.45 μmol L^{-1} to 9.78 μmol L^{-1} and mean SRP levels from 0.04 μmol L^{-1} to 1.8 μmol L^{-1}, altering mean starting DIN:TP molar ratios to 0.3, 86, and 5.8 for P, N, and C treatments respectively. The DIN:TP ratios generated represent the extremes of the historical range of observed environmental ratios found in Emerald Lake (roughly 0.2 to 200 molar DIN:TP; Sickman et al. 2003) and place N and P treatments in the range of respective P and N limitation according to the guidelines of Morris and Lewis (1988). The tenfold variability in ambient (Control treatment) DIN concentration between the two experiments was due to annual snowmelt flushing of nitrate and highlights the extreme seasonal variability in inorganic nutrient availability in montane lakes.

While the N treatment was not significantly different from the control through time in any of the biogeochemical response variables, P enrichment produced significant changes in both organic and inorganic nutrient concentrations (Fig 16). In the DARK experiment, the P treatment exhibited a significant increase in PN (Fig. 16). In the LIGHT experiment, while increases in PN under P enrichment were not significantly different from the control, there was a significant decrease in the ratio of PC:PN relative to the control, a trend also apparent but nonsignificant in the DARK experiment. PP increased significantly in the LIGHT (and nonsignificantly in the DARK; Fig. 16), exhibiting a final mean concentration of 0.28 μM, markedly higher than the 0.04 μM found in the control and N treatments, and leading to significant declines in the PC:PP ratio relative to the other treatments. A significant decline in DIN in the P treatment relative to the control during the LIGHT experiment was observed, along with a similar nonsignificant decline in DIN in the DARK experiment (Fig. 6). No significant treatment effect was found through time for the composition of the pool of dissolved organic matter in either experiment. All carboys in both experiments exhibited significant decreasing trends in ratios of dissolved to particulate organic

carbon through time, suggesting a transfer of organic material to larger size fractions through consumption processes (data not shown). Taken together, these results indicate that P enrichment significantly alters the nutrient composition of particulate organic material and the rate of nitrate utilization by the microbial community in Emerald Lake.

Microbial metabolic response

Bacterial production rates increased two- to four-fold in the LIGHT experiment and this increase was both rapid and sustained (Fig. 17) P-induced increase in bacterial production was not associated with a concomitant increase in cellular abundance in the P treatment, leading to a marked rise in cell-specific production (Fig. 17). In the DARK experiment, nutrient addition did not significantly alter the rate of DOC decline, the rate of increase in cellular abundance, or the cell-specific growth rate, although all carboys did experience a 4-fold increase in cellular abundance and a 3-5 μmol L^{-1} decline in DOC as expected in grazer-reduced dilution cultures (data not shown). Bacterial growth efficiency was highly variable among carboys, ranging from 10 to 65% and showing no significant difference between treatments (calculated as the change in cellular carbon concentration divided by the change in DOC during log phase growth using a conversion factor of 2 X 10^{-14} g C $cell^{-1}$; Lee & Fuhrman 1987).

No significant difference in the concentration of Chlorophyll a was observed between treatments in the LIGHT experiment, nor was there a significant trend in concentrations throughout the duration of the experiment (Fig. 17). The steady increasing trend in particulate carbon indicates that primary production was occurring throughout the experiment, but there was no significant effect of nutrient addition (Fig. 17).

Bacterial community response

Non-metric multidimensional scaling (NMS) of TRFLP fingerprint dissimilarity in the LIGHT experiment illustrates changes in bacterial community composition through time and the distinct emergence of a unique community in the P-enriched carboys after just one day (Fig. 18). The results of RM-MANOVA analyses comparing treatment effects on temporal variability of NMS axis values indicate that P-enrichment generated significant shifts in community composition through time along one NMS axis in both experiments (Fig. 18; DARK NMS results not shown). Stress for the two-dimensional NMS solutions was relatively low (11.55 for the LIGHT and 9.65 for the DARK experiment), indicating that community shifts were large relative to initial community heterogeneity.

In both LIGHT and DARK experiments P-enrichment produced communities which were significantly different from both the control and N-enriched treatments at the 99% confidence level by MRPP and began to differ significantly after just one day (Fig 18). N amendment did produce communities which were significantly different from the control on the second day of the DARK experiment and the second and sixth days of the LIGHT experiment, but overall there was no significant difference between the N and control treatments (A=0.03 and -0.01 respectively, $p > 0.05$). There was no significant difference between

treatments at the start of the DARK experiment, demonstrating that filtration and mixing manipulations were applied consistently between the treatments. In the MRPP analysis of the LIGHT experiment, communities were much more similar when grouped by date (A=0.27) than by treatment (A=0.07), although this was not true in the DARK experiment (A=0.10 and A=0.12, respectively), suggesting that the strong temporal trajectory of the unmanipulated light-exposed communities may be representative of the degree of temporal succession in the natural microbial assemblage. In the DARK experiment, bacterial phylotype richness (as measured by the number of distinct TRFLP fragments in each sample) declined significantly but increased by the end of the experiment (Fig. 18). Both bacterial richness and diversity (as calculated from the Shannon index) were significantly lower in the DARK experiment than in the light experiment, a trend not attributable to similar variability in the natural environment and therefore likely the result of the artificial environment generated by the darkened conditions and grazer removal.

Bacterial phylotype-specific responses

Figure 19 presents detailed trajectories of dominant phylotypes which exhibited temporal shifts significantly different from the control treatment as assessed by RM-MANOVA. At the broadest taxonomic level, P enrichment produced relative declines in two phylotypes of Actinobacteria (one lineage of Microbacteriaceae and one of Cellulomonadaceae) and relative increases in two phylotypes of Bacteriodetes (one lineage of Flavobacteriaceae and one of Crenotrichaceae) in both experiments. In addition, P enrichment produced a significant decline in the relative abundance of a single Cyanobacteria phylotype (a lineage of Prochlorales) in the LIGHT experiment. Responses by β-proteobacteria to P enrichment were mixed, with one lineage of Comamonadaceae declining significantly in the LIGHT experiment and three lineages giving different significant trends in the DARK experiment (significant decreases in two different lineages of the Comamonadaceae and a significant increase in one lineage of the Ralstoniaceae). There were no significant changes in specific phylotypes under N enrichment in the LIGHT treatment, but one β-proteobacteria phylotype (a distinct lineage of the Ralstoniaceae) increased significantly in the DARK experiment.

Conclusions

Role of bacterioplankton in lake metabolism

The primary productivity of Emerald Lake during the study period was typical of high-elevation lakes, in that increases in chlorophyll a concentration and rates of net primary production (NPP) throughout the ice-free period were driven by seasonal limnetic transitions linked to climatic variability. Both bacterial growth efficiency (BGE) and abundance increased significantly with these seasonal increases in NPP and chlorophyll, but bacterial production was temporally variable and not significantly related to BGE, NPP, or chlorophyll concentrations. Consequently, rates of bacterial respiration were inversely proportional to primary production, such that the system shifted from net heterotrophic to net autotrophic during periods of enhanced productivity. This relationship suggests that high-elevation lakes are generally maintained in a state of net heterotrophy during the bulk of the year due to relatively high rates of bacterial respiration during extended winter and spring periods of low primary production. These high rates of respiration are likely linked to decreased bacterial growth efficiency on terrestrially-derived dissolved organic matter which supports moderate to high rates of bacterial production throughout the year. With bacterial biomass averaging 40% of pelagic biomass and rates of production ranging from 1% to >500% of net primary production, we conclude that bacterioplankton comprise a key flux of energy and organic material through these ecosystems.

Phenology and biogeography of bacterioplankton communities and relationships between bacterioplankton and introduced salmonids

Analyses of bacterial biodiversity in Emerald Lake yielded 99 unique phylotypes, with statistical analyses suggesting actual diversity to be ~250. Bacterioplankton in Emerald Lake exhibited a distinct phenology, with recurring community types associated with spring snowmelt, ice-off, and fall overturn, each exhibiting significantly different phylogenetic structure and contributing to pooled β-diversity. Thermal stratification induced the emergence of unique communities each summer and increased community differentiation throughout the water column. Interannual variability in the timing of catchment snowmelt inputs and thermal stability largely predicted temporal distribution of nominal community types. Seasonal dynamics of phylotypes tracked via coupling of sequenced clones to fingerprint data roughly matched previous results from alpine lakes and were related to catchment solute inputs, stratification, and temperature. Surveys of lakes revealed high-elevation lake bacterioplankton displayed a distinct biogeographical structure, with community similarity declining with increasing distance within a given catchment. This observation supports suggests that macroecological principles of dispersal and isolation play a role in structuring communities of microorganisms, and indicates that bacterial community structure shifts across the landscape continuum. Introduced salmonids were not associated with any consistent community type, but fish presence and density were significant predictors of bacterial phylotype richness and Shannon diversity. Taken together, these results indicate a highly diverse bacterial community in

high-elevation Sierra Nevada lakes displaying dynamics seasonal and spatial patterning in response to environmental processes.

*Response of bacterioplankton to nutrient enrichment (*in situ *carboy experiments)*

Phosphorus enrichment generated rapid and significant impacts to prokarytic metabolism, bacterial community composition, and nutrient stocks in both experiments, but nitrate addition produced no significant responses in any of the key response variables. In whole-water enrichments exposed to light, phosphorus enrichment caused rapid (1 d) fourfold increases in prokaryotic production. This metabolic response was independent of phytoplankton responses to nutrient enrichment, which exhibited no significant change in chlorophyll or biomass relative to controls under either treatment. Phosphorus enrichment alone generated rapid and significant changes in bacterial community composition, including declines in the relative abundance of Actinobacteria and β-proteobacteria and increased dominance of Bacteriodetes. Nutrient enrichment produced no significant shift in bacterial abundance, growth efficiency, or DOC utilization in dark dilution cultures. Together these results point to strong phosphorus limitation of bacterioplankton in Emerald Lake, and suggest a direct response of the microbial community to nutrient deposition independent of increased eutrophication and phytoplankton productivity.

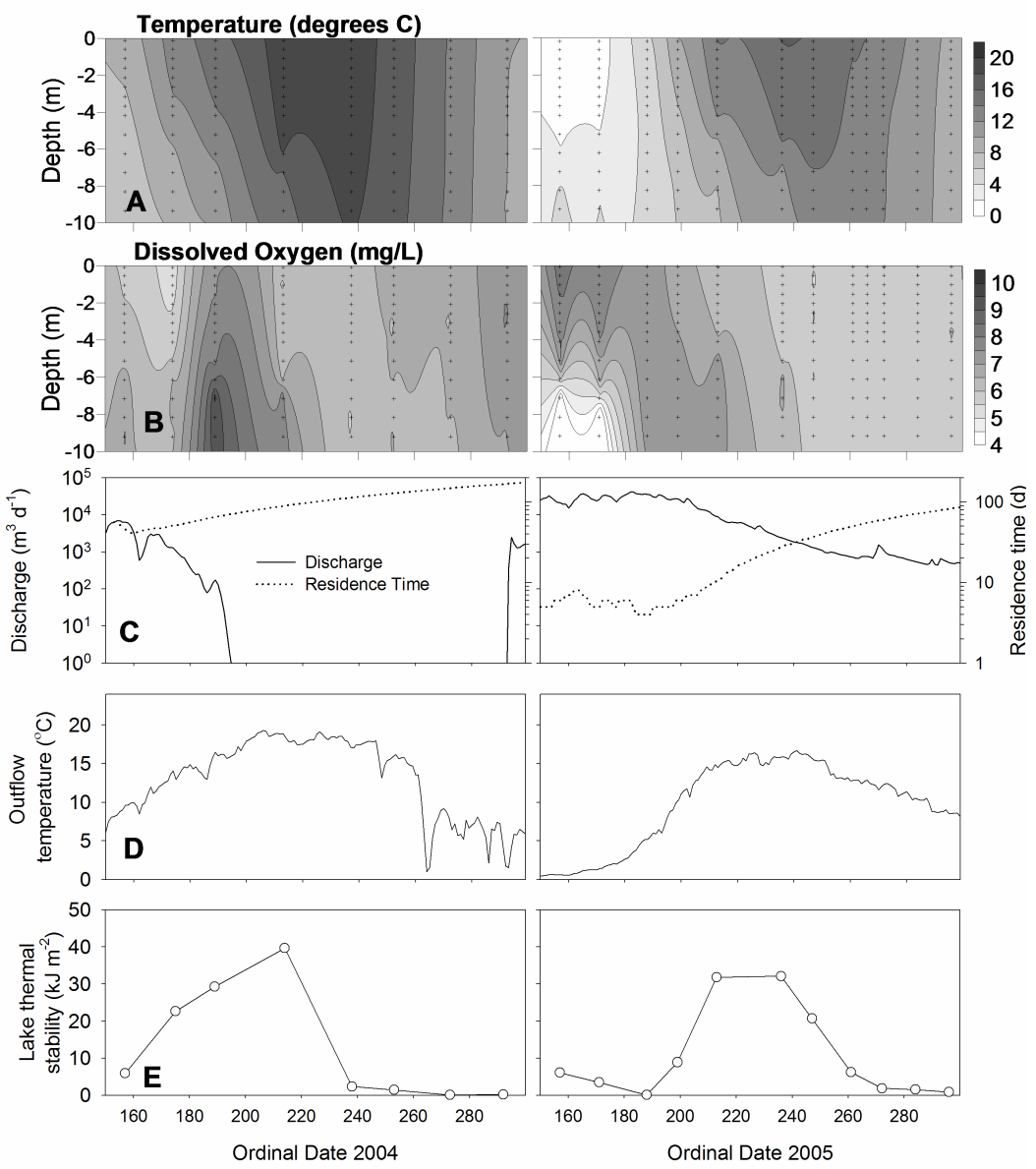

Figure 1: Physical characteristics of Emerald Lake during the growing seasons of 2004 and 2005. Panel A is a time-depth contour plot of temperature based on biweekly profiles. Panel B is the same measures with dissolved oxygen concentration contoured. Panel C is discharge measured via pressure transducer at the outflow weir with theoretical hydraulic residence time calculated as the number of cumulative discharge-days previous to each sampling point required to equal the volume of the lake. Panel D is the temperature measured continuously at the outflow. Panel E is is lake thermal stability from midday YSI55 temperature profiles conducted on each sampling date.

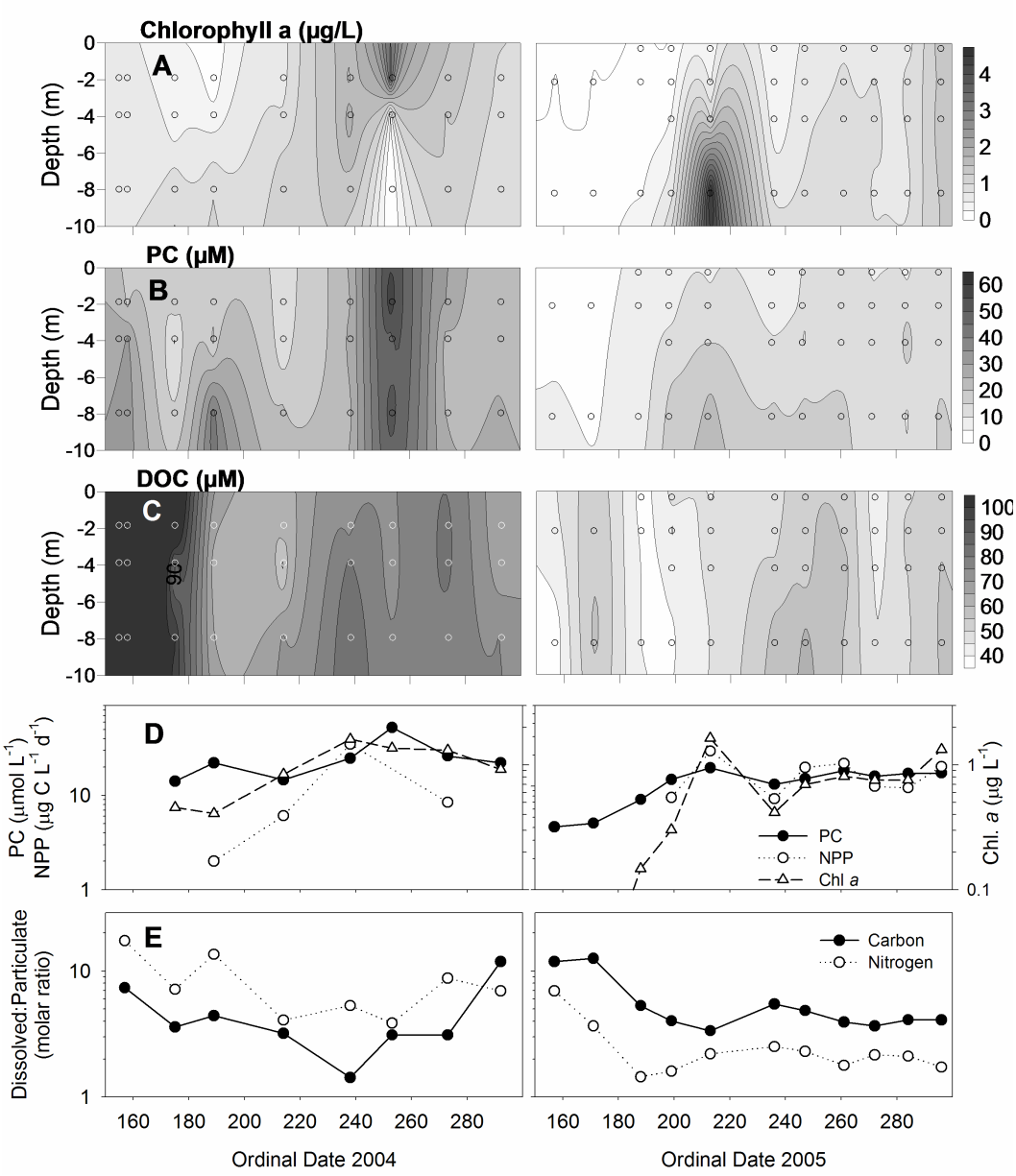

Figure 2: Measurements related to primary production in Emerald Lake during the growing seasons of 2004-2005. Panels A-C are contour plots of concentrations throughout the water column of the lake through time for chlorophyll *a*, particulate carbon (PC), and dissolved organic carbon (DOC), respectively. Panels D and E are depth-averaged values for various parameters relevant to estimating lake productivity, including PC, net primary production rate (NPP), chlorophyll *a*, and the ratio of dissolved to particulate organic carbon and nitrogen.

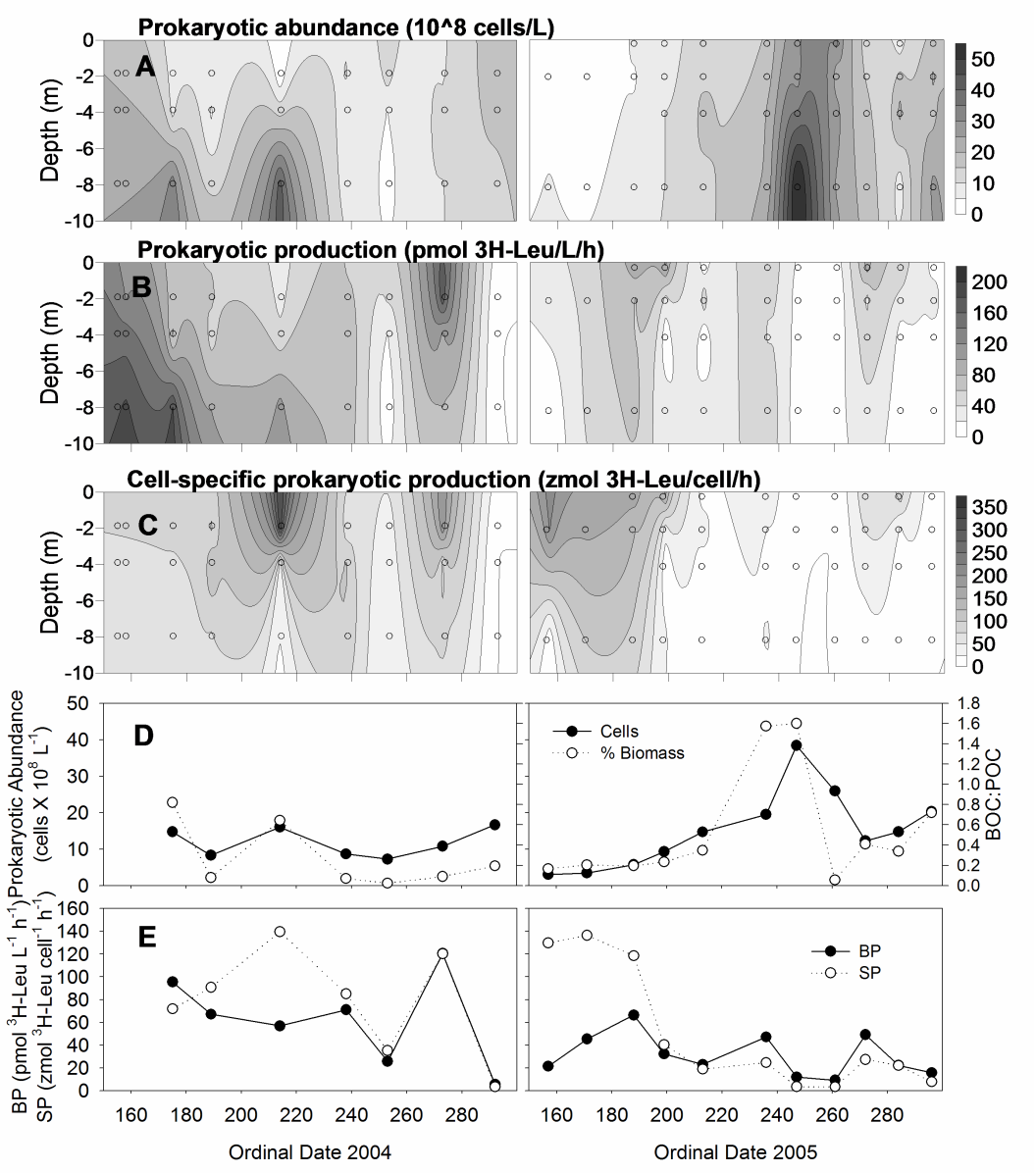

Figure 3: Bacterioplankton parameters measured in Emerald Lake during the growing seasons of 2004-2005. Panels A-C are production rates and stocks of prokaryotes throughout the water column through time. Panels D and E are depth-averaged values for the above parameters. Details are discussed in the text. BOC:POC is the ratio of bacterial carbon to non-bacterial particulate organic carbon, and is represented in the legend as % Biomass [bacterial].

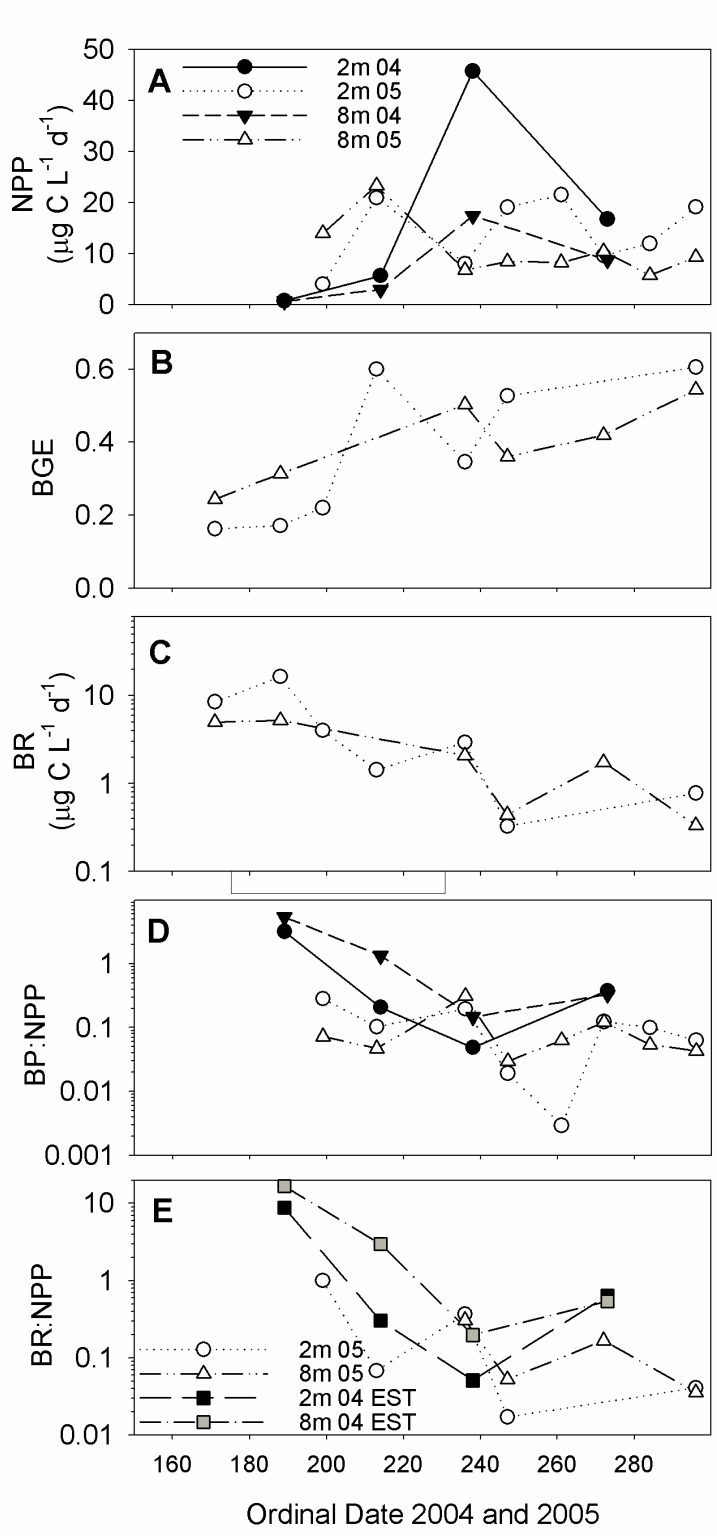

Figure 4: Metabolic parameters of Emerald Lake plankton at 2 and 8 m depth 2004-05. White symbols are 2005, dark are 2004, circles are 2 m depth, triangles are 8 m. Bacterial growth efficiency (BGE) was not measured in 2004, therefore BR:NPP values for 2004 (squares in Panel E) were estimated from BP:NPP in 2004 (see Results).

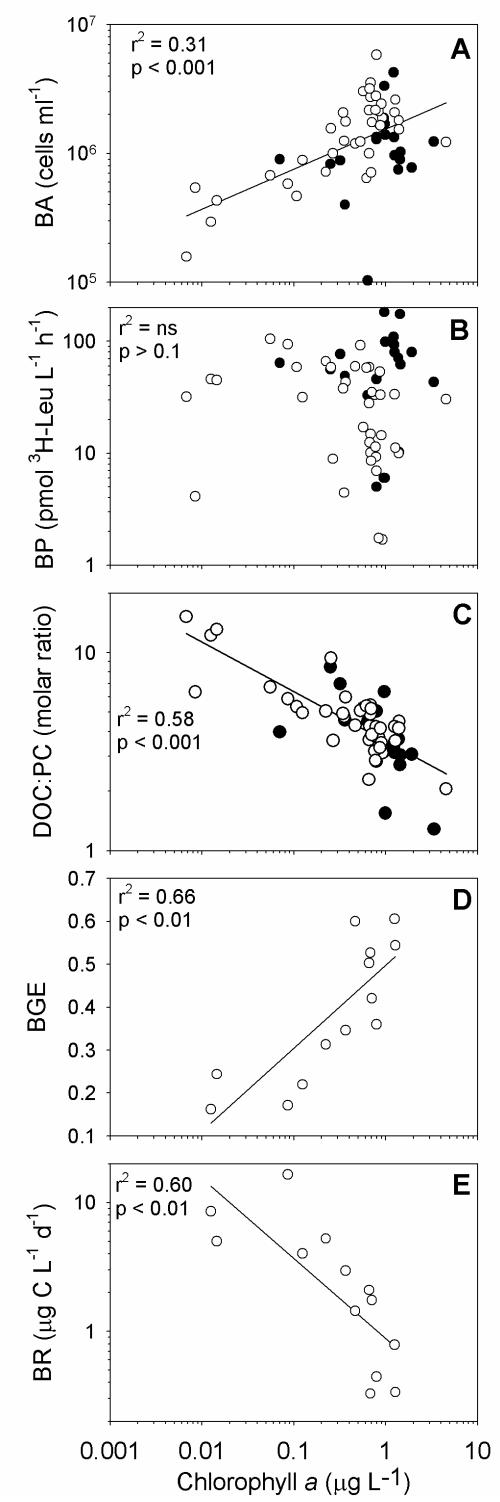

Figure 5: Relationships between metabolic variables and chlorophyll *a* throughout the water column of Emerald Lake 2004-05. White symbols are values from 2005, dark are from 2004. Regressions using data from two years were first analyzed via ANCOVA and regression slopes were not significantly different between years ($p > 0.20$ for interaction effect X*Year by Y), although 2004 data were nonsignificant for Panel A and B.

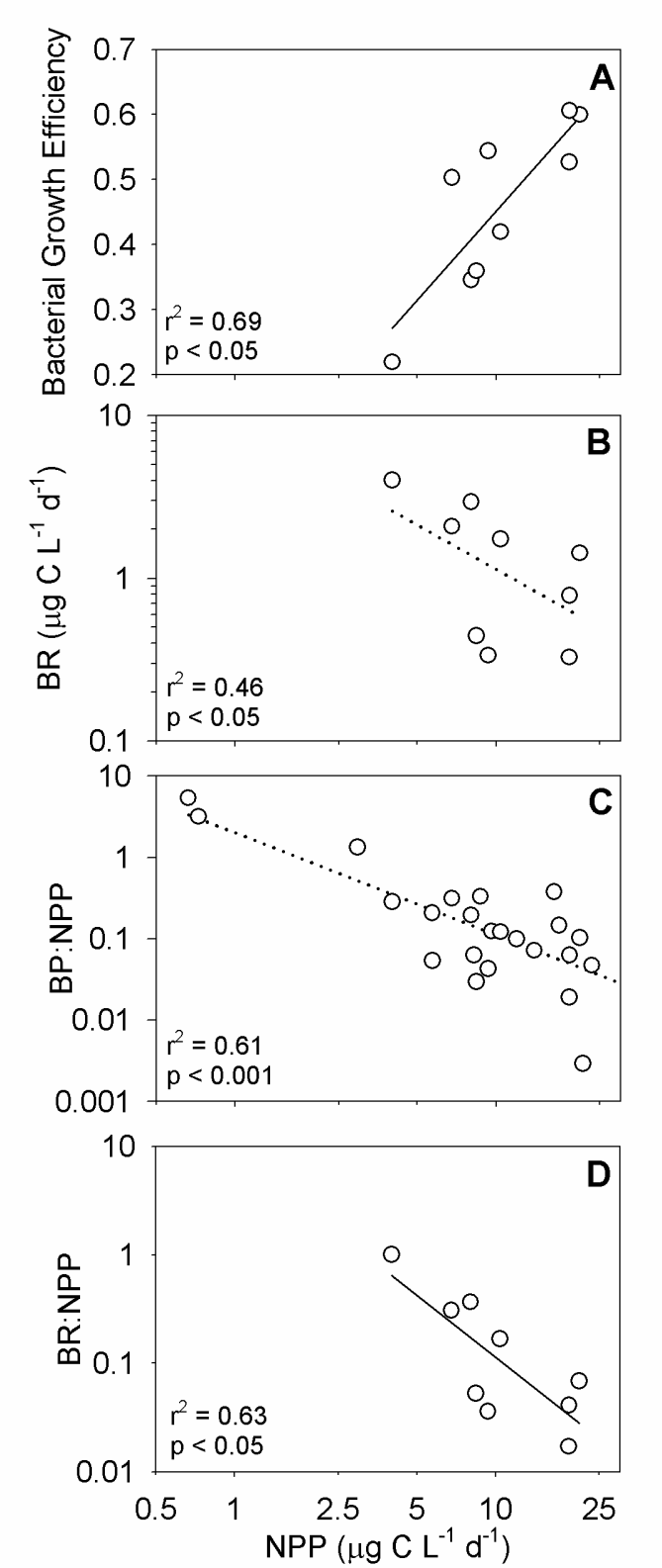

Figure 6: Relationships among metabolic indicators within Emerald Lake. Panels A, B, and D contain data from 2005 only. Panel D contains data from both 2004 and 2005. Ratios of BP:NPP and BR:NPP are key metrics of the relative contribution of bacterial metabolism to ecosystem productivity and net metabolic balance (see text).

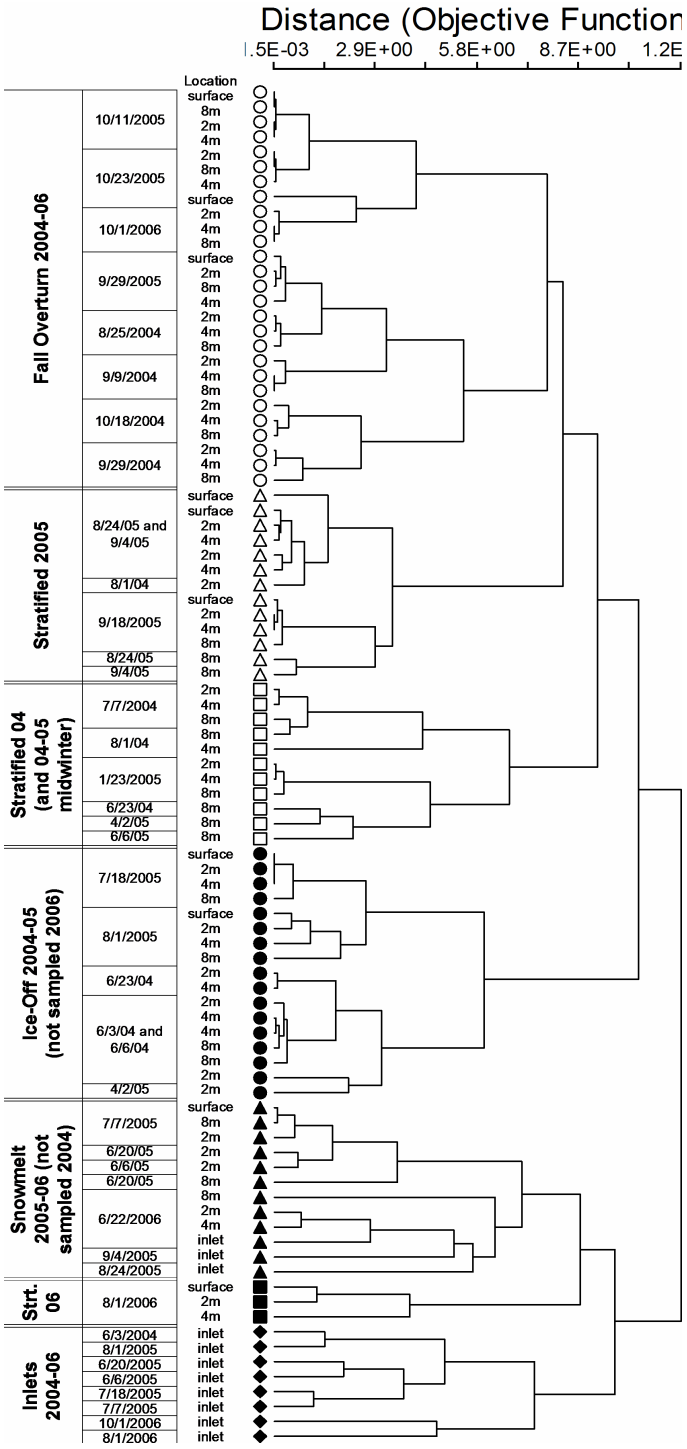

Figure 7. Cluster dendrogram of TRFLP fingerprint data from DNA samples collected in Emerald Lake and its inlet 2004 - 2006. Dendrogram is based on Sorensen distances between TRFLP samples clustered using the flexible-β method (β = -0.25) and scaled according to Wishart's objective function. Samples are coded according to seven groups selected in order to minimize within-group distances and maximize variance explained using elbow criteria. Samples groups are named based on interpretation of temporal similarity and lake mixing status. Groupings are significantly different (MRPP; A = 0.28, all pairwise $p << 0.001$, within-group dissimilarity < 50% except inlets = 0.62).

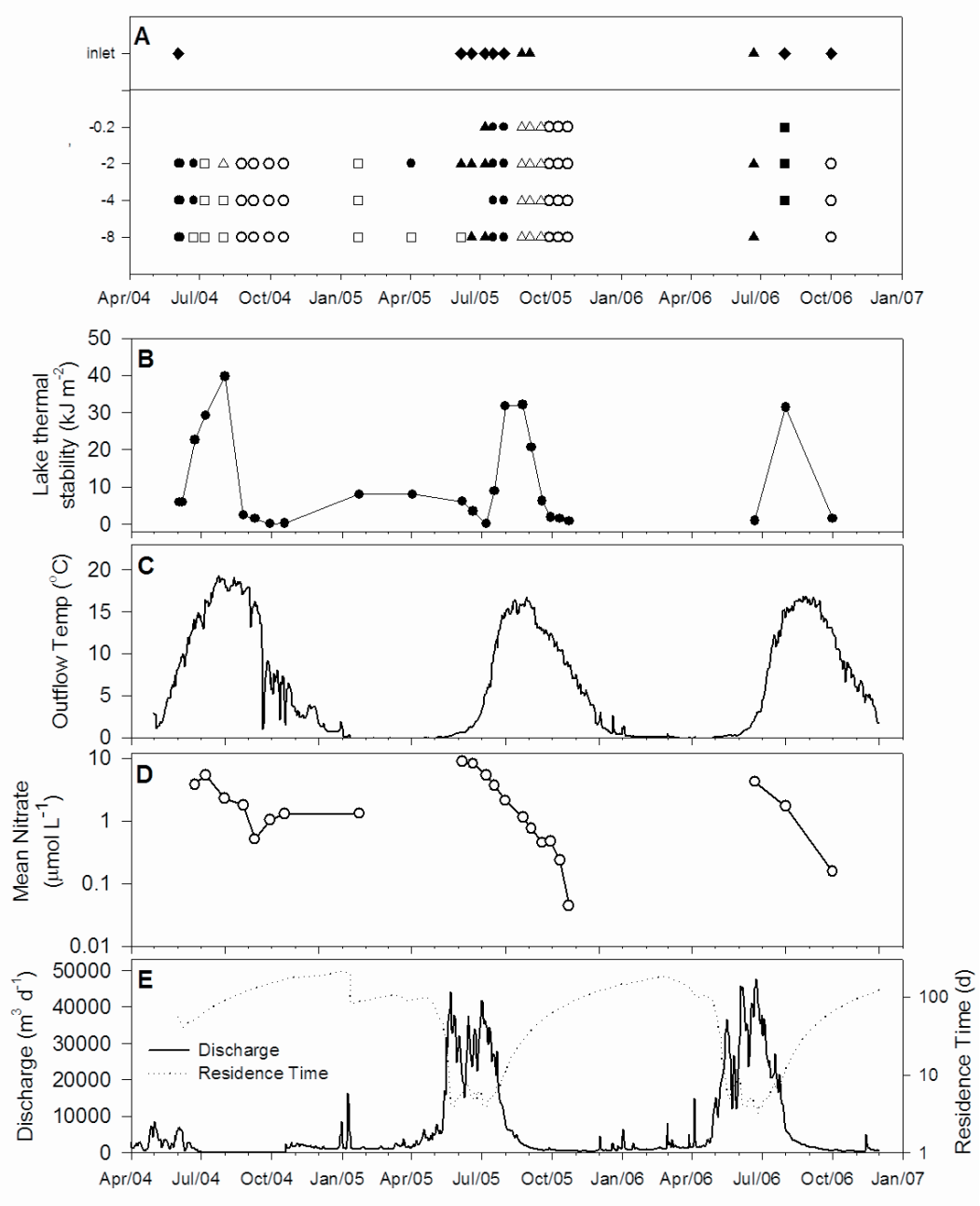

Figure 8. Bacterial community types of Emerald Lake in relation to physical variables. Panel A is the distribution of TRFLP community fingerprint types (defined in Fig. 7) through time throughout the water column (including inlet samples). Panel B is lake thermal stability (Schmidt Stability Index) calculated from temperature profiles taken at each sampling timepoint. Panel C is the temperature of the outflow. Panel D is the depth-averaged water column nitrate concentration. Panel E is the discharge rate measured via pressure transducer at the weir and calculated theoretical hydraulic residence time.

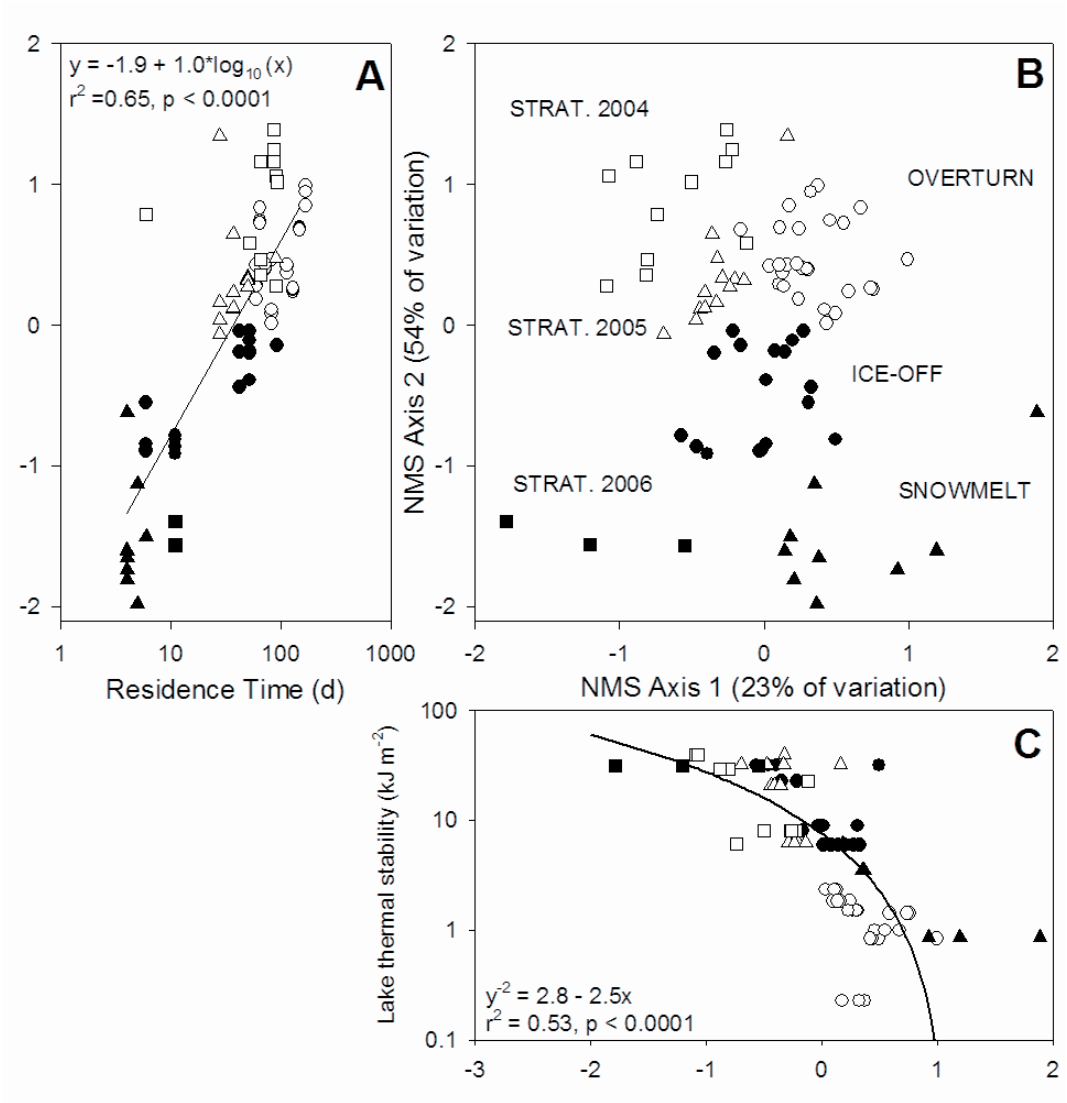

Figure 9. NMS ordination of TRFLP fingerprint samples in relation to environmental descriptors in Emerald Lake 2004-2006. Panel B is the two-dimensional NMS solution with symbols coded and labeled according to groups defined in Fig. 7. Panels A and C are regressions of physical parameters which best fit the two axes of community variability, suggesting possible abiotic regulators of community structure. Inlet samples were excluded from this analysis for clarity.

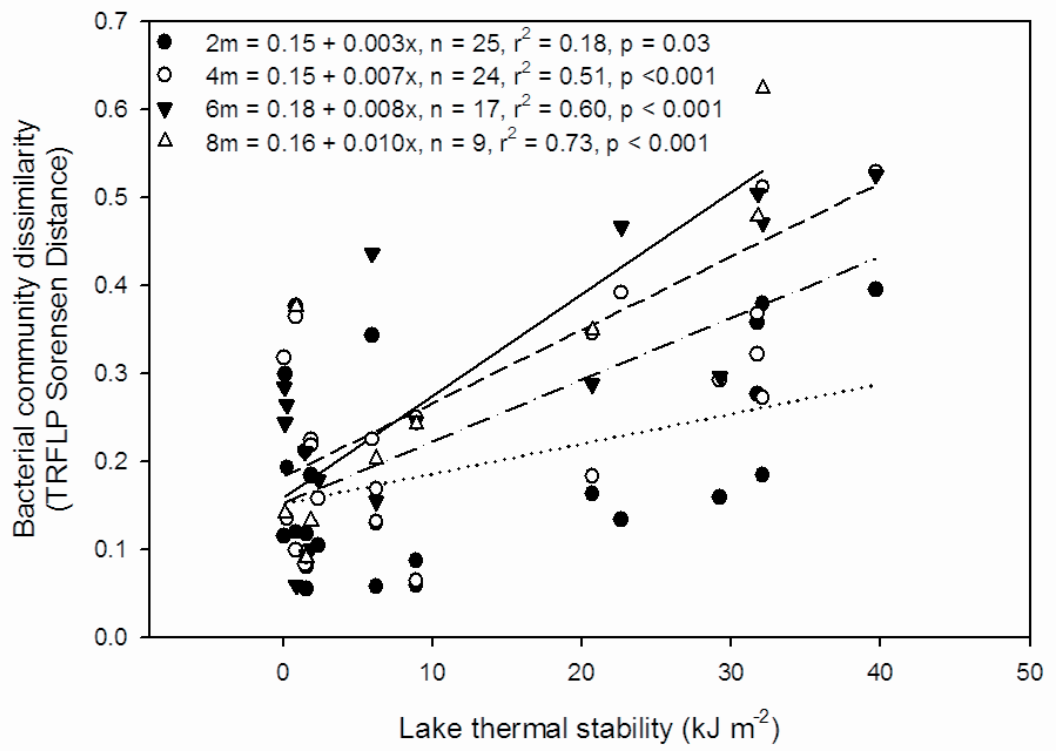

Figure 10. Relationship between lake thermal stability (measured as Schmidt stability index) and pairwise bacterial community dissimilarity (measured as Sorensen distance between TRFLP samples) for various water-column distances. Each data point represents the community distance between two samples within the water column of Emerald Lake during the ice-free periods of 2004 and 2005. Symbols are coded as follows according to the pairwise Δz: 2m distance includes surface-2m and 2m-4m, 4m distance includes surface-4m and 4m-8m, 6m distance is 2m-8m, and 8m distance is surface-8m. Surface samples were only collected in 2005. Note that community dissimilarity increases significantly with increased stratification and the slope of the relationship increases with increased distance in the water column. Epilimnetic samples 2m apart show a weak and only marginally significant increase in community distance with the onset of stratification, likely due to limited diurnal and wind-driven mixing.

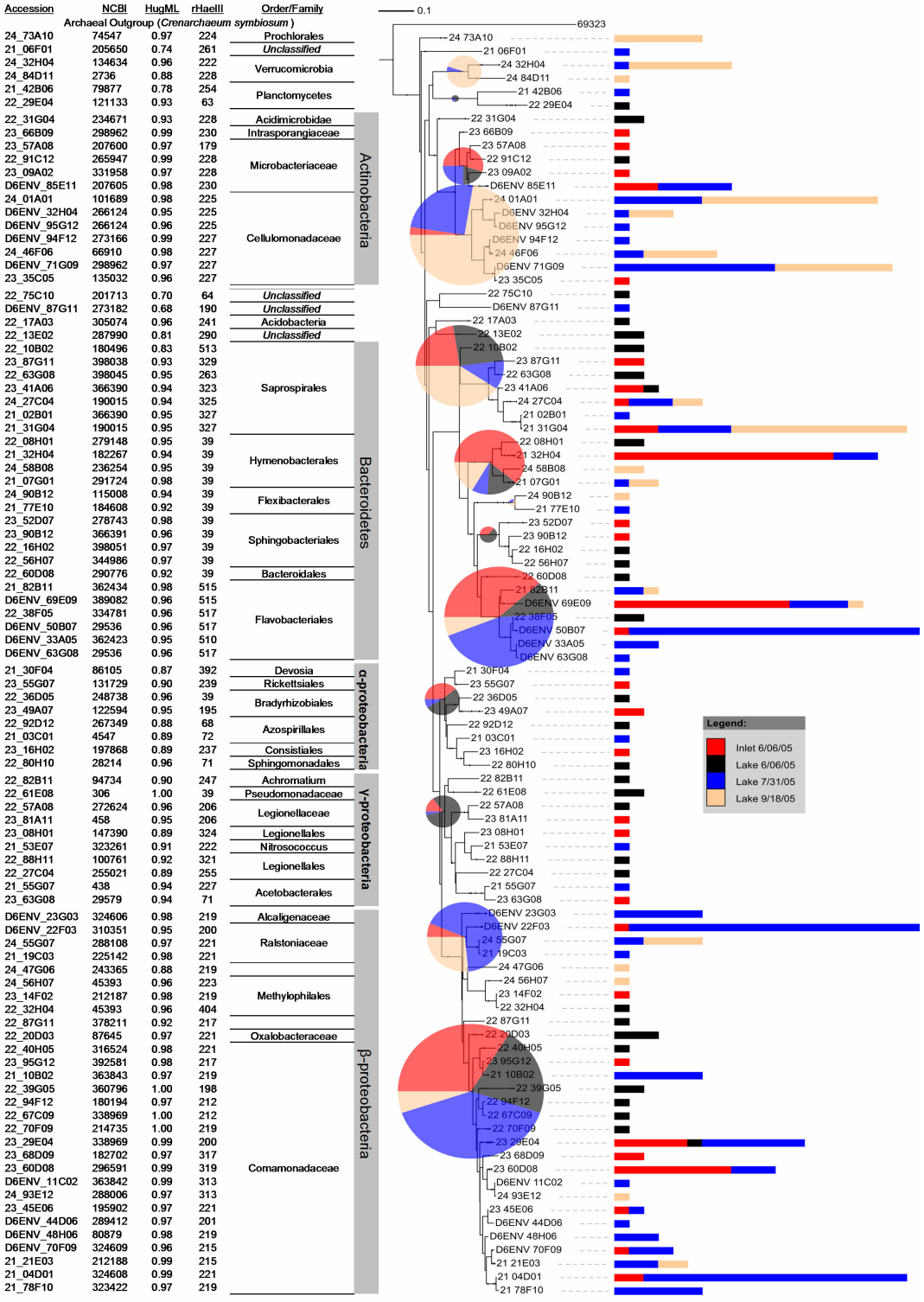

Figure 11. Phylogenetic tree of unique clones from Emerald Lake pooled across four sampling dates in 2005. See text for details. Colored bars extending to the right of each clone ID represent the number of duplicate clones found in each environment. Clones were summed within clades to construct a pie chart of relative clone distribution among environments (see Methods) and clades were labeled according to the lowest common taxonomic label.

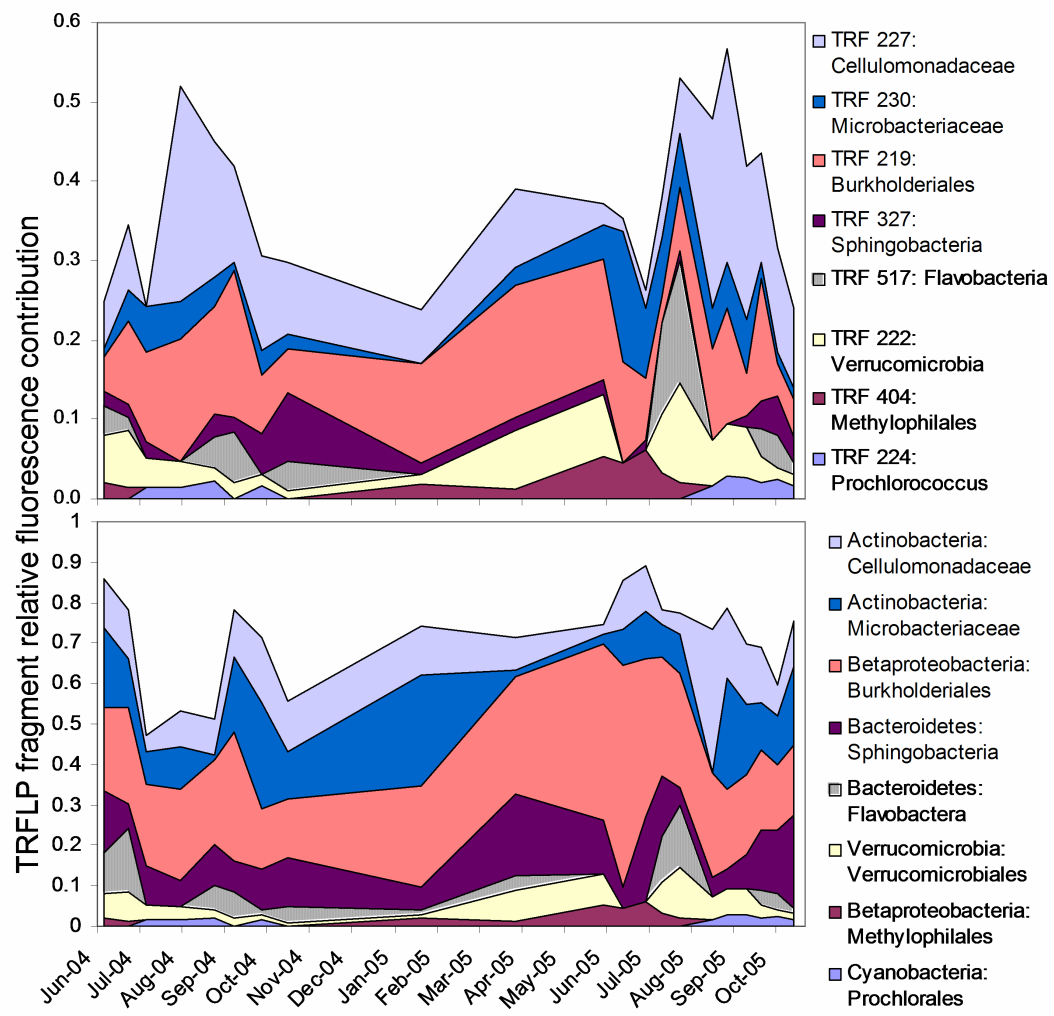

Figure 12. Temporal dynamics of relative TRFLP fluorescence of dominant fragments and clades from 2m depth in Emerald Lake 2004-2005. The top panel displays dynamics of specific fragment lengths which generally include 1-3 unique phylotypes and are clade-specific. The lower panel displays dynamics of family-level clades including multiple related phylotypes.

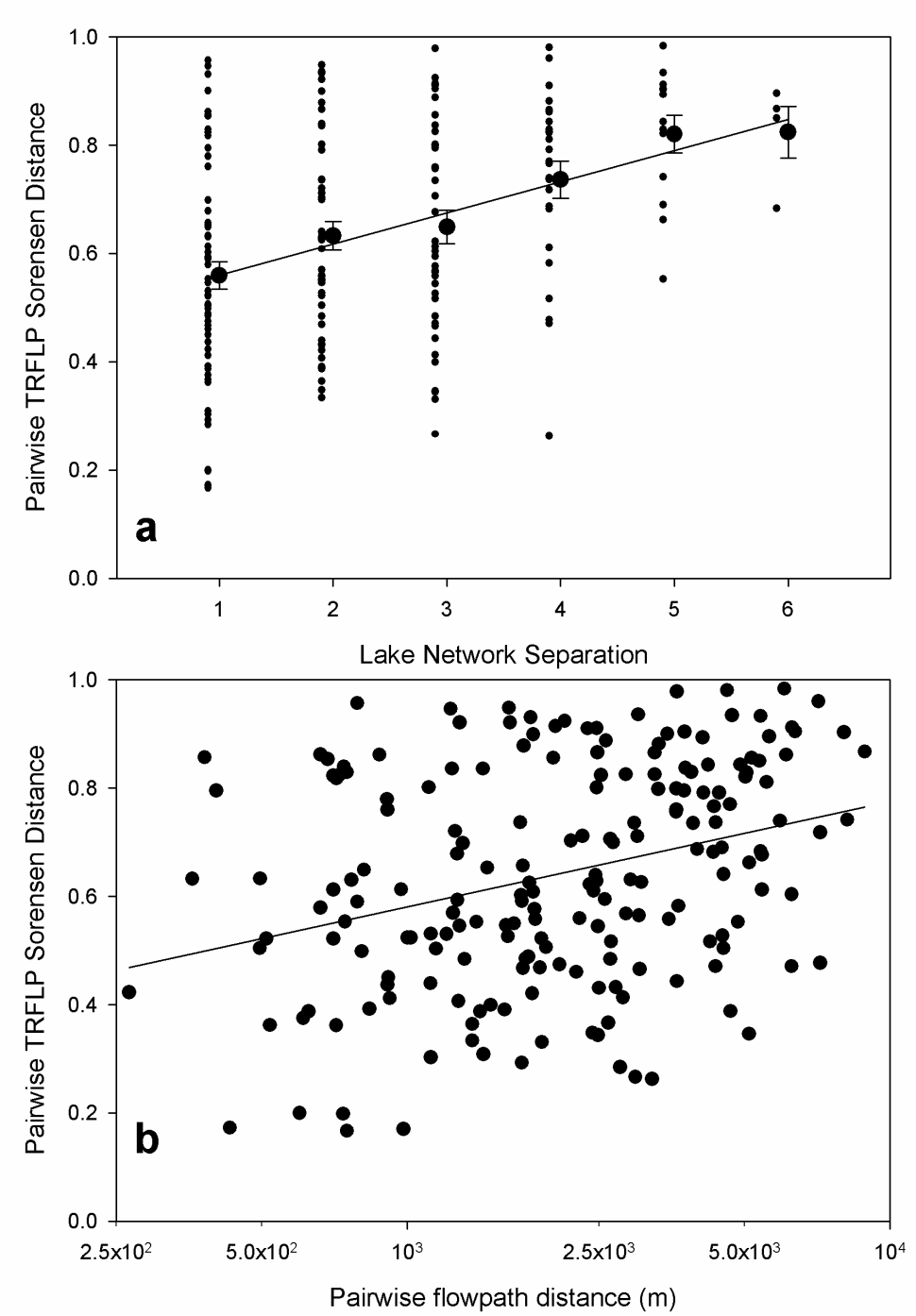

Figure 13: Relationship between lake physical separation and community compositional similarity within 14 catchments across the Sierra Nevada. Lake network separation in panel 5a is the difference between LNN values of any two lakes. Points in panel 5a are staggered for visualization and the mean is displayed as a larger symbol ± standard error. Pairwise flowpath distance is the distance between two points within a single catchment. Samples not connected by hydraulic flow (i.e., in separate catchments) were not compared. Regressions are $p < 0.01$, $n = 197$ with Panel 5a: $r^2 = 0.15$ and Panel 5b $r^2 = 0.10$. Regression through the means in panel A exhibits $r^2 = 0.96$, but we feel this is a misleading interpretation of the data.

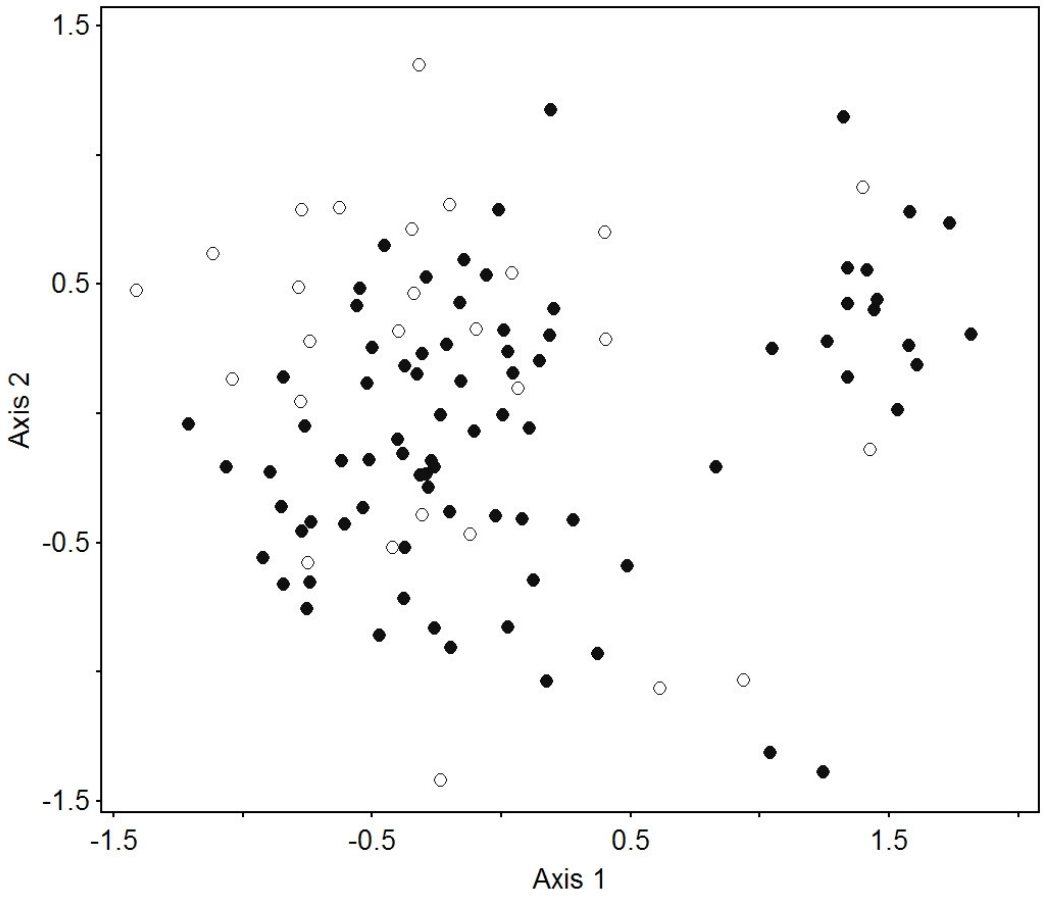

Figure 14: Non-metric multidimensional scaling ordination of lake bacterial fingerprint samples (TRFLP) from the 2006 Sierra survey. White circles are fishless lakes (CPUE < 1.5) and dark circles are lakes with fish (CPUE > 1). Grouping of samples by the presence or absence of introduced salmonids yielded no significant difference between groups. Analysis results are the same with differing CPUE cutoffs defining fishless lakes (See text).

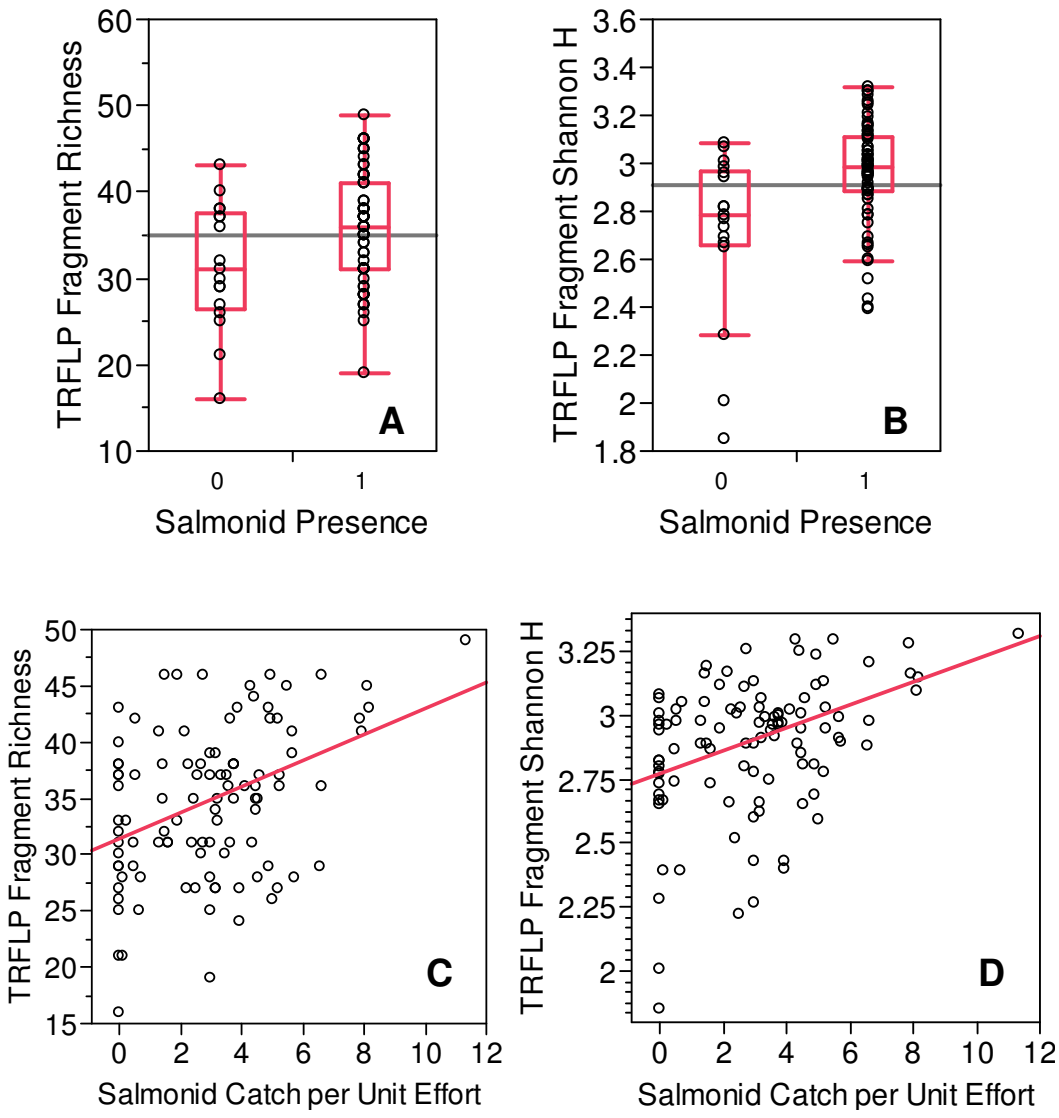

Figure 15: Relationship between density and presence/absence of introduced salmonids and diversity indices of bacterioplankton among lakes throughout the Sierra Nevada. Panels A and B display quantiles (box/whiskers) and pooled means (solid line) of lake TRFLP richness and Shannon diversity index (H') values between lakes with CPUE salmonid densities of 0 (fish absent) or > 0 (fish present). Two-tailed t-tests with unequal variance yield $p < 0.001$ in both cases and for various fishless classifications of CPUE < 1.5 and CPUE < 2.5. Panels C and D are regressions of CPUE as a predictor of lake TRFLP richness or H'. Equations and statistics are as follows: Richness = 31.5 + 1.16*CPUE, H' = 2.78 + 0.045*CPUE, both $r^2 = 0.17$, n = 88, $p < 0.0001$.

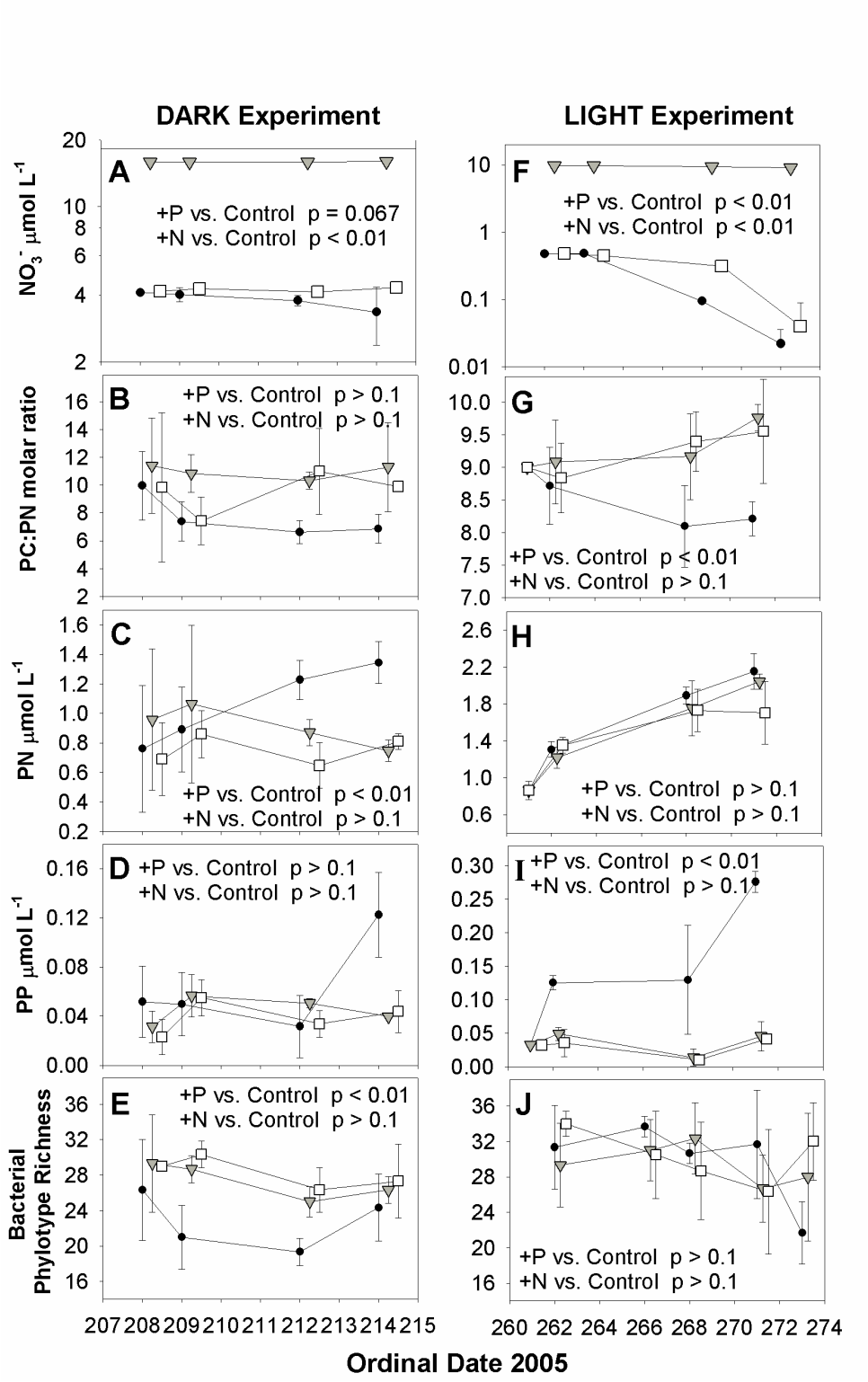

Figure 16: Biogeochemical responses in nutrient enrichment experiments. Temporal dynamics of selected response variables which exhibited significant treatment effects during the Dark and Light experiments conducted in 2005 in Emerald Lake (see text). Black circles are P, grey triangles are N, white squares are Control treatments. Bars are ± std. dev. P-values are treatment effects tested by RM-MANOVA.

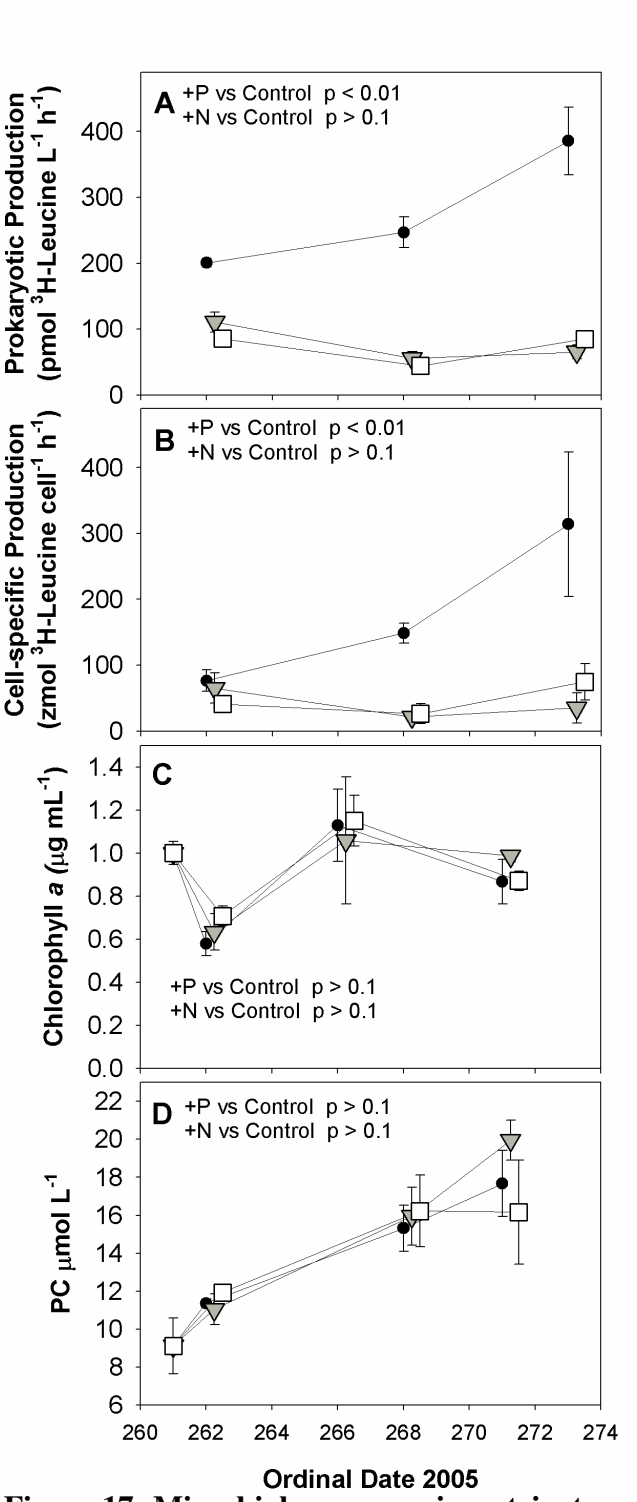

Figure 17: Microbial responses in nutrient enrichment experiments. Temporal dynamics of selected metabolic response variables which were measured only during the Light experiment. Black circles are P, grey triangles are N, white squares are Control treatments. Bars are ± standard deviation. P-values are treatment effects tested by RM-MANOVA.

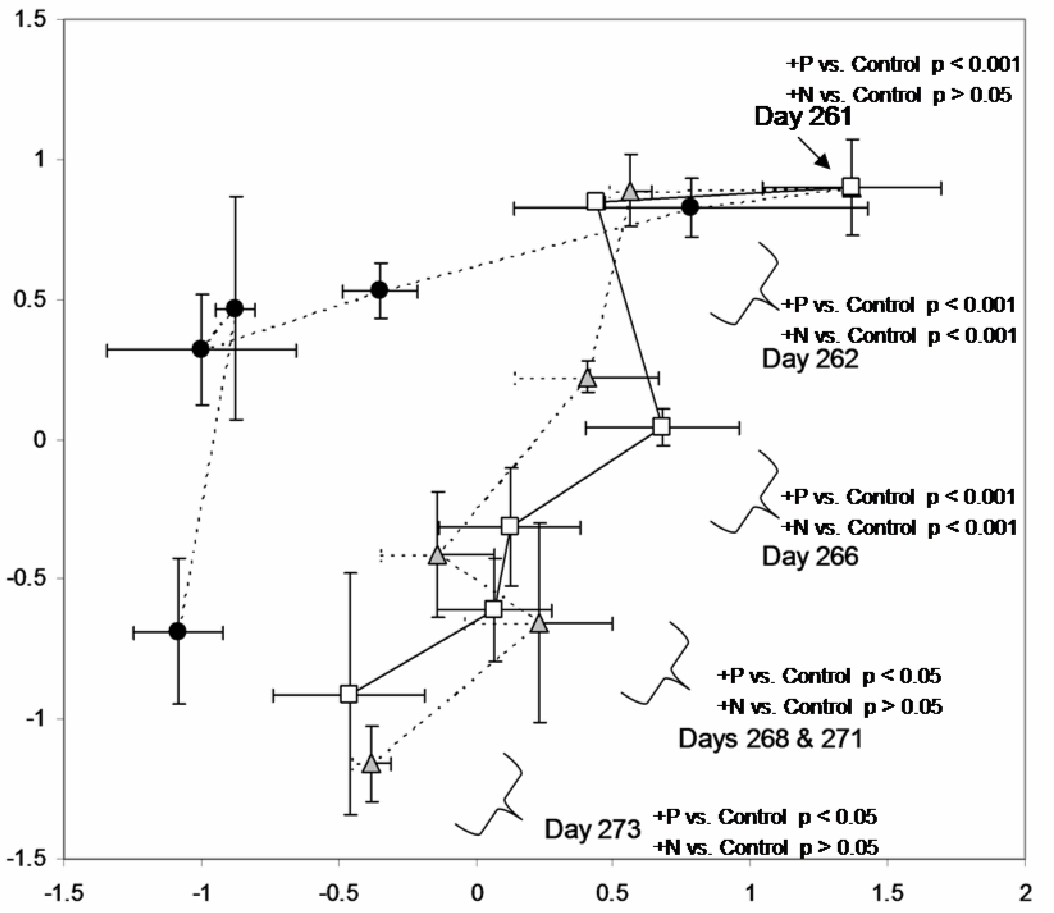

Figure 18: Shifts in bacterial community composition in response to nutrient amendment. NMS ordination plot (dimensionless axes) of changes in bacterial community composition during the Light experiment. Treatment triplicates were averaged at each timepoint as in above figures. Becase all carboys followed the same temporal trend of changes in community composition sampling dates are labeled according to their ordination position using brackets. Black circles are P, grey triangles are N, white squares are Control treatments. Bars are ± standard deviation. P-values are likelihoods of communities grouping into treatments by chance as determined by multiresponse permutation (MRPP).

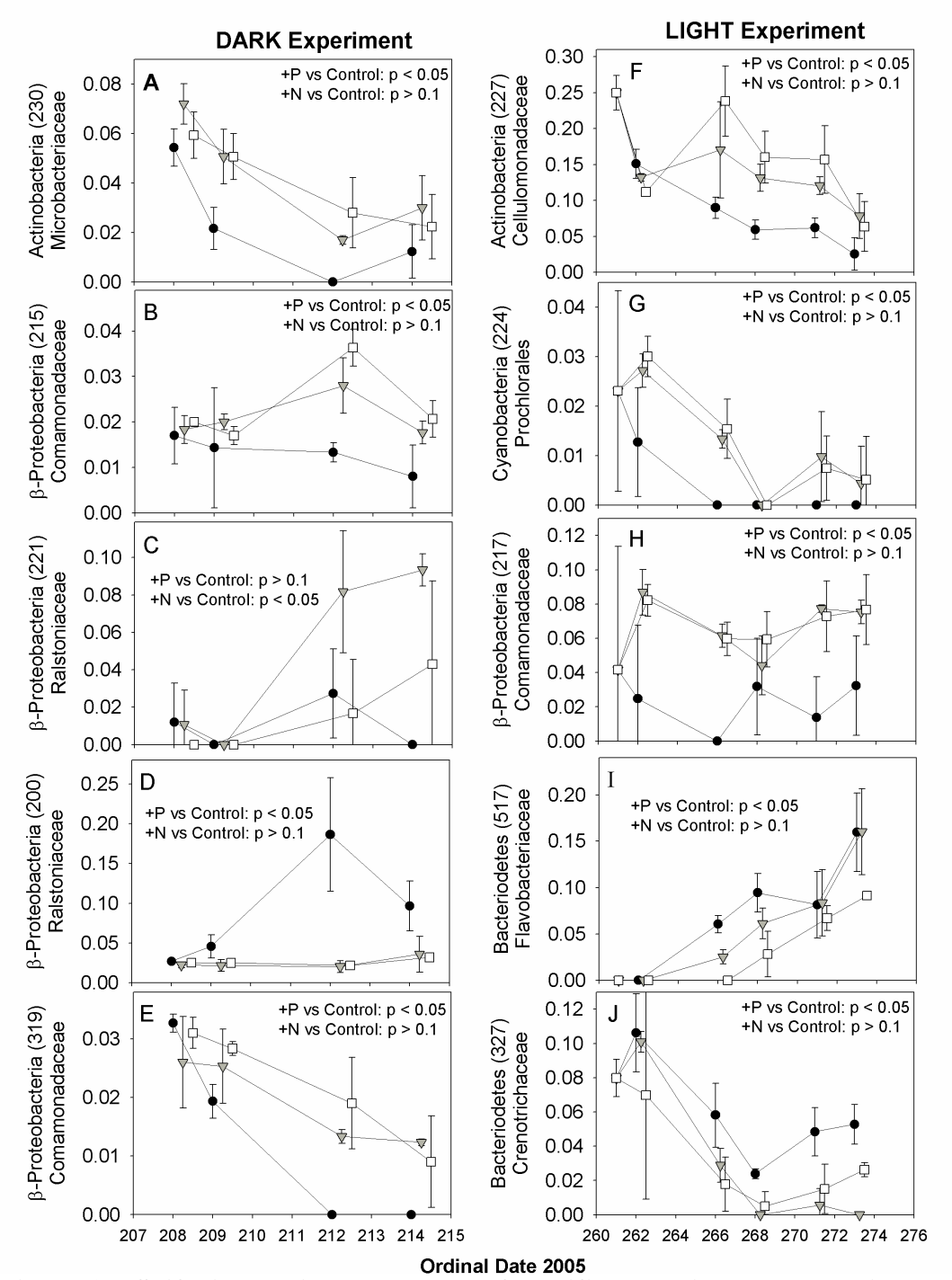

Figure 19: Shifts in relative abundance of specific bacterial phylotypes in response to nutrient amendment. Temporal dynamics of selected phylotype relative abundances which exhibited significant treatment effects during the two experiments. Y-axis values are relative abundance of each phylotype determined by electropherogram peak area in TRFLP fingerprint data. Black circles are P, grey triangles are N, white squares are Control treatments. Bars are ± standard deviation. P-values are for treatment effects tested by RM-MANOVA.

References

Brown, M. V., M. S. Schwalbach, I. Hewson, and J. A. Fuhrman. 2005. Coupling 16S-ITS rDNA clone libraries and automated ribosomal intergenic spacer analysis to show marine microbial diversity: development and application to a time series. Environ. Microbiol. **7:** 1466-1479.

Carlson, C. A., H. W. Ducklow, D. A. Hansell, and W. O. Smith. 1998. Organic carbon partitioning during spring phytoplankton blooms in the Ross Sea polynya and the Sargasso Sea. Limnol. Oceanogr. **43:** 375-386.

Cole, J. J. 1999. Aquatic microbiology for ecosystem scientists: New and recycled paradigms in ecological microbiology. Ecosystems **2:** 215-225.

Cole, J. J., S. Findlay, and M. L. Pace. 1988. Bacterial production in fresh- and salt-water ecosystems: A cross-system overview. Mar. Ecol.-Prog. Ser. **43:** 1-10.

Del Giorgio, P. A., and J. J. Cole. 1998. Bacterial growth efficiency in natural aquatic systems. Annu. Rev. Ecol. Syst. **29:** 503-541.

Desantis, T. Z. and others 2006a. NAST: a multiple sequence alignment server for comparative analysis of 16S rRNA genes. Nucleic Acids Res. **34:** W394-W399.

---. 2006b. Greengenes, a chimera-checked 16S rRNA gene database and workbench compatible with ARB. Appl. Environ. Microbiol. **72:** 5069-5072.

Ducklow, H. W. 2000. Bacterial production and biomass in the oceans. *In* D. L. Kirchman [ed.], Microbial ecology of the oceans. Wiley-Liss.

Felsenstein, J. 2005. PHYLIP (Phylogeny Inference Package). Distributed by the author. Department of Genome Sciences, University of Washington, Seattle.

Grant, A., and L. A. Ogilvie. 2004. Name that microbe: rapid identification of taxa responsible for individual fragments in fingerprints of microbial community structure. Mol. Ecol. Notes **4:** 133-136.

Hall, T. A. 1999. BioEdit: a user-friendly biological sequence alignment editor and analysis program for Windows 95/98/NT. Nucl. Acids. Symp. Ser. **41:** 95-98.

Hama, T. and others 1983. Measurement of photosynthetic production of a marine phytoplankton population using a stable C-13 isotope. Mar. Biol. **73:** 31-36.

Hewson, I., and J. A. Fuhrman. 2006. Improved strategy for comparing microbial assemblage fingerprints. Microbial Ecology **51:** 147-153.

Huber, T., G. Faulkner, and P. Hugenholtz. 2004. Bellerophon: a program to detect chimeric sequences in multiple sequence alignments. Bioinformatics **20:** 2317-2319.

Idso, S. B. 1973. On the concept of lake stability. Limnol. Oceanogr. **18**: 53-71.

Kling, G. W., G. W. Kipphut, and M. C. Miller. 1992. The flux of CO_2 and CH_4 from lakes and rivers in Arctic Alaska. Hydrobiologia **240:** 23-36.

Knapp, R. A., and K. R. Matthews. 2000. Non-native fish introductions and the decline of the mountain yellow-legged frog from within protected areas. Conserv. Biol. **14:** 428-438.

Lee, S., and J. A. Fuhrman. 1987. Relationships between biovolume and biomass of naturally derived marine bacterioplankton. Appl. Environ. Microbiol. **53:** 1298-1303.

Letunic, I., and P. Bork. 2007. Interactive Tree Of Life (iTOL): an online tool for phylogenetic tree display and annotation. Bioinformatics **23:** 127-128.

Liu, W. T., T. L. Marsh, H. Cheng, and L. J. Forney. 1997. Characterization of microbial diversity by determining terminal restriction fragment length polymorphisms of genes encoding 16S rRNA. Appl. Environ. Microbiol. **63:** 4516-4522.

Mccune, B., and M. J. Mefford. 2006. PC-ORD. Multivariate Analysis of Ecological Data.

Melack, J. M., S. D. Cooper, and T. M. Jenkins. 1989. Chemical and biological characteristics of Emerald Lake and the streams in its watershed, and the responses of the lake and streams to acidic deposition, p. 377. California Air Resources Board and University of California, Santa Barbara.

Melack, J. M., and J. L. Stoddard. 1991. p. 503-530. *In* D. F. Charles [ed.], Acidic Deposition and Aquatic Ecosystems: Case Studies. Springer-Verlag.

Morris, D. P., and W. M. Lewis. 1988. Phytoplankton nutrient limitation in colorado mountain lakes. Freshw. Biol. **20:** 315-327.

Morris, R. M., K. L. Vergin, J. C. Cho, M. S. Rappe, C. A. Carlson, and S. J. Giovannoni. 2005. Temporal and spatial response of bacterioplankton lineages to annual convective overturn at the Bermuda Atlantic Time-series Study site. Limnol. Oceanogr. **50:** 1687-1696.

O'Brien, R. G., and M. K. Kaiser. 1985. MANOVA method for analyzing repeated measures designs: An extensive primer. Psychol. Bull. **97:** 316-333.

Porter, K. G., and Y. S. Feig. 1980. The use of DAPI for identifying and counting aquatic microflora. Limnol. Oceanogr. **25:** 943-948.

Schmidt, W. 1928. Über Temperatur und Stabilitätsverhältnisse von Seen. Geogr. Ann. **10**: 145-177.

Sickman, J. O. 2001. Comparative analyses of nitrogen biogeochemistry in high-elevation ecosystems. Doctoral dissertation: University of California, Santa Barbara.

Sickman, J. O. and others 2003a. Mechanisms underlying export of N from high-elevation catchments during seasonal transitions. Biogeochemistry **64:** 1-24.

Sickman, J. O., J. M. Melack, and D. W. Clow. 2003b. Evidence for nutrient enrichment of high-elevation lakes in the Sierra Nevada, California. Limnol. Oceanogr. **48:** 1885-1892.

Simon, M., and F. Azam. 1989. Protein content and protein synthesis rates of planktonic marine bacteria. Mar. Ecol.-Prog. Ser. **51:** 201-213.

Smith, D. C., and F. Azam. 1992. A simple economical method for measuring bacterial protein synthesis rates in sea water using tritiated leucine. Marine Microbial Food Webs **6:** 107-114.

Smith, R. C., K. S. Bakers, and P. Dustan. 1981. Fluorometric techniques for the measurement of oceanic chlorophyll in the support of remote sensing. Ref. Rep. Scripps Institution of Oceanography (La Jolla, California) **81-17:** 1-14.

Soranno, P. A. and others 1999. Spatial variation among lakes within landscapes: Ecological organization along lake chains. Ecosystems **2:** 395-410.

Sørensen, T. J. 1948. A method of establishing groups of equal amplitude in plant sociology based on similarity of species content and its application to analysis of the vegetation of the Danish Commons. Biologiske Skrifter **5:** 1-34.

Stepanauskas, R., M. A. Moran, B. A. Bergamaschi, and J. T. Hollibaugh. 2003. Covariance of bacterioplankton composition and environmental variables in a temperate delta system. Aquat. Microb. Ecol. **31:** 85-98.

Stothard, P. 2000. The sequence manipulation suite: JavaScript programs for analyzing and formatting protein and DNA sequences. Biotechniques **28:** 1102-+.

Valderrama, J. C. 1981. The simultaneous analysis of total nitrogen and total phosphorus in natural waters. Mar. Chem. **10:** 109-122.

Yannarell, A. C., and E. W. Triplett. 2005. Geographic and environmental sources of variation in lake bacterial community composition. Appl. Environ. Microbiol. **71:** 227-239.

Yu, Y. N., M. Breitbart, P. Mcnairnie, and F. Rohwer. 2006. FastGroupII: A web-based bioinformatics platform for analyses of large 16S rDNA libraries. BMC Bioinformatics **7**.